Cross Sections for Collisions of Electrons and Photons with Nitrogen Molecules

Y. Itikawa, M. Hayashi,[a] A. Ichimura, K. Onda, K. Sakimoto, K. Takayanagi

Institute of Space and Astronautical Science, Komaba, Meguroku, Tokyo 153, Japan

M. Nakamura

Institute of Physics, University of Tsukuba, Ibaraki 305, Japan

H. Nishimura

Department of Physics, Niigata University, Niigata 950-21, Japan

and

T. Takayanagi

Department of Physics, Sophia University, Chiyodaku, Tokyo 102, Japan

Received July 23, 1985; revised manuscript received January 22, 1986

Data have been compiled on the cross sections for collisions of electrons and photons with nitrogen molecules (N_2). For electron collisions, the processes considered are: total scattering, elastic scattering, momentum transfer, excitations of rotational, vibrational and electronic states, dissociation, and ionization. Ionization and dissociation processes are discussed for photon impact. Cross section data selected are presented graphically. Spectroscopic and other properties of the nitrogen molecule are summarized. The literature was surveyed through the end of 1984, but some more recent data are included when useful.

Key words: cross section data; electron collision; molecular properties; nitrogen molecule; photodissociation; photoionization.

Contents

[a] Visiting Professor 1984–1985. Permanent address: Nagoya Institute of Technology, Nagoya 466, Japan.

1. Introduction

Collisions of electrons and photons with nitrogen molecules are of significance in many areas, since nitrogen is one of the most fundamental molecules. They play an essential role, for instance, in ionospheric and auroral phenomena in the Earth's upper atmosphere and in a variety of gaseous discharge processes. Almost 20 years ago, Takayanagi and Takahashi[117] made a compilation of data on electron collisions with nitrogen molecules. They gave a comprehensive set of cross sections based on the data then available and some theoretical estimates of their own. Since that time remarkable progress has been made in atomic collision physics and a large volume of new pertinent data have become available. The present paper is the complete update of the previous compilation with an addition of the data on photon collisions.

The literature has been surveyed through the end of 1984, but some more recent data are taken considered as far as available to the present authors. After a critical review of the original papers, a selection of data was made on the basis of the reliability of the method used to obtain those data. Often experimental data are preferred, but theoretical values are selected when no reliable measurements are available. The resulting cross sections are shown graphically. In a few cases, where a large number of data are reported, the best values have been determined and shown to be recommended for use. In cases where it is difficult to decide which data are better, multiple, not unique, sets of data are shown. The disagreement indicates their reliability. When only one set of data has been reported, the set is presented here with caution. In all the cases, absolute values of the cross sections in the units of cm^2 are plotted against the electron energy in eV or the photon wavelength in Å.

For electron collisions, an attempt has often been made to deduce a comprehensive set of cross sections from an analysis of swarm experiment (e.g., Ref. 38). Though providing valuable information, such a method has a difficulty in deriving a unique set of the cross sections, especially at higher electron energies. In the present paper, no use is made of the data based on the swarm analysis, except for momentum-transfer and vibrational cross sections at the energies less than 1.8 eV.

To keep the total number of pages reasonable, some restrictions have been applied to the present data compilation. Cross sections are considered only for the collisions with a nitrogen molecule in its electronic ground state. Collisions with the molecular ions are excluded, though some spectroscopic data are given for N_2^+, $N_2^{+\,+}$, and N_2^- in Sec. 2. No data are presented on the angular dependence of the cross section, i.e., the differential cross section with respect to angular variables. The energy of electrons and photons is limited, in general, to less than 1 keV. Finally, the list of references includes only the literature cited in the text, figures, and tables.

Because of the nature of this paper as a data compilation, no detailed discussions of the physics of the collision processes are given. For the detailed discussion, see the original papers cited or review articles and books (for recent reviews, see Refs. 68, 73, and 124; for recent books, see Refs. 32, 76, 80, and 106).

In the next section (Sec. 2) properties of the nitrogen molecule are summarized to help the understanding of the collision processes. In Sec. 3, photon collision data are given. In Secs. 4–9, the data on electron collisions are presented. Finally in Sec. 10, a summary is given and future problems are discussed.

2. Properties of the Nitrogen Molecule

2.1. Energy Levels

a. Electronic Energy Levels of N_2, N_2^+, $N_2^{+\,+}$, and N_2^-

Molecular constants and energy levels were critically reviewed by Lofthus and Krupenie.[74] Their paper shows detailed potential energy curves for N_2 and N_2^+. Spectroscopic constants are summarized also by Suchard and Melzer[115] and by Huber and Herzberg.[62] Michels[81] calculated many highly excited states not reported in those reviews. Here we give lists of electronic states with some important characteristic information selected from the above references. Table 2.1 shows the major states of N_2. Table 2.2 lists the additional states whose existence is predicted by the theoretical calculation.[81] The states of N_2^+ are tabulated in Table 2.3.

Energy levels of $N_2^{+\,+}$ are known fragmentarily (see Ref. 121 for a recent calculation). From photofragment spectroscopy, Cosby *et al.*[37] concluded that the ground state ($X\,^1\Sigma_g^+$, $v = 0$) of $N_2^{+\,+}$ lies 4.8 ± 0.2 eV above the lowest dissociation limit, $N^+(^3P) + N^+(^3P)$. This suggests that the ground state of $N_2^{+\,+}$ is located at 43.6 eV above $N_2X\,^1\Sigma_g^+$ ($v = 0$). This is a little higher than the ionization energies measured for the production of $N_2^{+\,+}$ (for instance, 42.7 ± 0.5 eV by Agee *et al.*[3]).

The system, $e + N_2$, has many resonance states (corresponding to temporary negative ion states of N_2). Those are shown in Fig. 2.1. Details of the resonances are reviewed, for instance, by Schulz.[101]

Table 2.1. Major electronic states of N_2 (All values are taken from the review by Lofthus and Krupenie (1977)[a] unless otherwise stated in the footnotes.)

State	T_0[b] (eV)	Diss. products[c]	D^0[d] (eV)	$\Delta E_{vib}(0\text{-}1)$[e] (eV)	B_0[f] (10^{-4}eV)	r_e[g] (Å)	Footnote
$o_4\,^1\Pi_u$	15.145			0.2262	2.150	1.178(r_0)	h
$o_4(^3\Pi_u)$	15.011			0.2390			h
$c_5'\,^1\Sigma_u^+$	(14.359)[u]			0.2755	1.668		h,i
$c_4\,^1\Pi_u$	14.328			0.2705	2.388	1.116	h,j
$*\,^1\Delta_g$	14.304	$^2D^o+^2P^o$	1.415	~0.211	2.174	1.169	k
$y\,^1\Pi_g$	14.143			0.2271	2.146	1.177	l
$k\,^1\Pi_g$	14.100			0.2706	2.410	1.109	
$x\,^1\Sigma_g^-$	14.036			0.2317	2.157	1.173	
$a''(^1\Sigma_u^-$ or $^1\Delta_u)$	13.804						
$o_3\,^1\Pi_u$	13.107			0.2424	2.144	1.178	m
$H\,^3\Phi_u$	(13.0)[u]	$^2D^o+^2D^o$	(1.508)[u]	0.1115	1.336	1.488	
$c_4'\,^1\Sigma_u^+$	12.935			0.2671	2.405	1.104	n
$c_3\,^1\Pi_u$	12.912			0.2682	2.371	1.112	o
$b'\,^1\Sigma_u^+$	12.854	$^2D^o+^2P^o$	2.952	0.0932	1.427	1.439	
$D\,^3\Sigma_u^+$	(12.841)[u]				2.431	1.108(r_0)	
$b\,^1\Pi_u$	12.500	$^2D^o+^2D^o$	2.027	0.0787[h]	1.794	1.279	
$a''\,^1\Sigma_g^+$	12.255				2.372	1.122	p
$C'\,^3\Pi_u$	12.101	$^4S^o+^2D^o$	(0.041)[u]	0.0898[h]	1.301	1.515(r_0)	q
$E\,^3\Sigma_g^+$	(11.875)[u]	"	0.268	0.2709	2.390	1.118	
$C''\,^3\Pi_u$	(11.6)[u]	"	0.56	0.0553	1.40	1.45	r
$C\,^3\Pi_u$	11.032	"	1.111	0.2476	2.251	1.149	
$G\,^3\Delta_g$	(10.8)[u]	"	(1.339)[u]	0.0920	1.141	1.611	
$A'\,^5\Sigma_g^+$	(9.66)[u]	$^4S^o+^4S^o$	(0.101)[u]	~0.081		(1.55)[u]	s
$w\,^1\Delta_u$	8.8895	$^2D^o+^2D^o$	5.637	0.1904	1.844	1.269	
$a\,^1\Pi_g$	8.5489	"	5.978	0.2066	1.994	1.220	
$a'\,^1\Sigma_u^-$	8.3987	"	6.128	0.1868	1.825	1.275	
$B'\,^3\Sigma_u^-$	8.1647	$^4S^o+^2P^o$	5.170	0.1851	1.816	1.278	
$w\,^3\Delta_u$	7.3622	$^4S^o+^2D^o$	4.781	0.1833		1.28	t
$B\,^3\Pi_g$	7.3532	"	4.790	0.2114	2.019	1.2126	
$A\,^3\Sigma_u^+$	6.1688	$^4S^o+^4S^o$	3.590	0.1777	1.792	1.2866	
$X\,^1\Sigma_g^+$	0	"	9.759	0.28887	2.4668	1.0977	

[a] Energy units are changed with the conversion factor 1 cm^{-1} = 1.23985 x 10^{-4} eV.

[b] Energy of the lowest vibrational state relative to N_2 $X\,^1\Sigma_g^+$ (v=0).

[c] Electronic states of the dissociation products, N + N.

[d] Dissociation energy.

[e] Energy difference between the vibrational states with v=0 and 1.

[f] Rotational constant for the lowest vibrational state (v=0).

[g] Equilibrium internuclear distance. In some cases, the mean value for the lowest vibrational state (denoted by r_0) is indicated.

[h] From Huber and Herzberg (1979).

[i] Suchard and Melzer (1976) identify this state as $e'\,^1\Sigma_u^+$.

[j] Suchard and Melzer (1976) identify this state as $e\,^1\Pi_u$.

[k] Huber and Herzberg (1979) give T_0 = 14.272 eV.

[l] Suchard and Melzer (1976) give T_0 = 14.155 eV.

[m] Suchard and Melzer (1976) and Huber and Herzberg (1976) give T_0 = 13.103 eV.

[n] Huber and Herzberg (1979) give T_0 = 12.949 eV.

[o] Huber and Herzberg (1979) give T_0 = 12.943 eV.

[p] Suchard and Melzer (1976) give T_0 = 12.278 eV.

[q] Huber and Herzberg (1979) give T_0 = 12.096 eV.

[r] Huber and Herzberg (1979) give T_0 = 11.45 eV. The values of D^0, E_{vib}, B_0 and r_e are from Michels (1981).

[s] This is identified as $^5\Sigma^-$ by Suchard and Melzer (1976).

[t] Suchard and Melzer (1976) give T_0 = 7.5080 eV.

[u] ( ) means uncertain.

Table 2.2. Electronic states of N_2 not indicated in Table 2.1 but theoretically predicted by Michels (1981).[a]

State	T_0[b] (eV)	Diss. products[c]	D^0[d] (eV)	$\Delta E_{vib}(0\text{-}1)$[e] (eV)	B_0[f] (10^{-4}eV)	r_e[g] (Å)	Footnote
$^1\Phi$ (A3dδg)	15.09(T_e)[h]					1.19	i
$^1\Sigma_g^-$	14.07 14.17(T_e)	$^2P^o+^2D^o$	1.65	0.0779	0.95	1.75	
$^3\Phi_u$ (A3dδg)	14.12(T_e)					1.20	i
$x''\,^1\Sigma_g^+$ (A3pπu)	14.06(T_e)					1.20	i
$^1\Phi_u$	13.89 13.99(T_e)	$^2D^o+^2D^o$	0.64	0.0867	1.36	1.47	j
$^3\Sigma_g^-$ (A3pπu)	13.80(T_e)					1.20	i
$^3\Pi_g$ (A4pσu)	13.74(T_e)					1.19	i
$^1\Delta_g$	13.56 13.66(T_e)	$^2D^o+^2D^o$	0.96	0.0948	1.16	1.60	
$^3\Delta_g$ (A3pπu)	13.62(T_e)					1.18	i
$^1\Sigma_g^+$	13.53 13.65(T_e)	$^2D^o+^2D^o$	0.99	0.0519	1.0	1.70	
$^3\Sigma_g^+$ (A3pπu)	13.51(T_e)					1.20	i
$G\,^3\Pi_u$ (X3pπu)	12.72(T_e)					1.23	i
$F\,^3\Pi_u$ (A3sσg)	12.59(T_e)					1.31	i
$^1\Gamma_g$	12.40 12.49(T_e)	$^2D^o+^2D^o$	2.13	0.1038	1.16	1.60	k
$^3\Sigma_g^-$	11.94 12.04(T_e)	$^4S^o+^2P^o$	1.39	0.0964	1.15	1.61	l
$^5\Sigma_g^+$	11.87 11.98(T_e)	$^4S^o+^2D^o$	0.27	0.0853	0.66	2.13	
$^1\Sigma_g^+$	10.02 10.09(T_e)	$^2D^o+^2D^o$	4.51	0.1436	1.21	1.57	m

[a-g] The same as a-g in Table 2.1.

[h] T_e is the minimum of the potential curve.

[i] Read from the graph in Michels (1981).

[j] Taken from Table III of Michels (1981). His graph shows a little different values (T_e~13.74 eV, r_e~1.55 Å).

[k] Taken from Table III of Michels (1981). His graph shows a little different value of T_e (~12.2 eV).

[l] Taken from Table III of Michels (1981). His graph shows T_e of a little lower value than 12.0 eV.

[m] Taken from Table III of Michels (1981). His graph shows T_e of a little lower value than 10.0 eV.

Table 2.3. Electronic states of N_2^+ (All values are taken from the review by Lofthus and Krupenie (1977)[a] unless otherwise stated in the footnotes.)

State	T_0[b] (eV)	Diss. products[c]	D^0[d] (eV)	$\Delta E_{vib}(0\text{-}1)$[e] (eV)	B_0[f] (10^{-4}eV)	r_e[g] (Å)	Footnote
$G^2\Sigma_g^+$	(39.622)[k]	$^4S^o+^3P^o$		repulsive			h
$C^2\Sigma_u^+$	23.583	$^4D^o+^3P$	3.094	0.2544	1.872	1.263[i]	
$D^2\Pi_{gi}$	22.049	$^4S^o+^3P$	2.245	0.1099	1.368	1.471	
($a^4\Sigma_u^+$)	(18.750)[k]			(0.294)[k]	(2.559)[k]		h
$B^2\Sigma_u^+$	18.751	$^4S^o+^3P$	5.543	0.2943	2.558	1.078	
$A^2\Pi_{ui}$	16.699		7.595	0.2323	2.155	1.174	
$X^2\Sigma_g^+$	16.581		0.713	0.2896	2.363	1.116	j

[a] Energy units are changed with the conversion factor 1 cm^{-1} = 1.23985 x 10^{-4} eV.

[b] Energy of the lowest vibrational state relative to N_2 $X^1\Sigma_g^+$ (v=0).

[c] Electronic states of the dissociation products. N + N^+.

[d] Dissociation energy.

[e] Energy difference between the vibrational states with v=0 and v=1.

[f] Rotational constant for the lowest vibrational state (v=0).

[g] Equilibrium internuclear distance.

[h] From Huber and Herzberg (1979).

[i] Mean value (r_0) for the lowest vibrational state.

[j] The lowest state of N_2^+.

[k] ( ) means uncertain.

b. Vibrational–Rotational Levels of the Electronic States

Vibrational–rotational energies are given by

$$E_{vJ} = E_v + B_v J(J+1) - D_v J^2(J+1)^2, \qquad (2.1)$$

where v and J are the vibrational and rotational quantum numbers, respectively. The numerical values of E_v, B_v, D_v are listed in Table 2.4 for the electronic ground state ($X\ ^1\Sigma_g^+$) of N_2. Vibrational–rotational energies for other states can be roughly estimated from ΔE_{vib} (0→1) and B_0 given in Tables 2.1–2.3.

Table 2.4. Vibrational-rotational energy of the ground electronic state ($X^1\Sigma_g^+$) of N_2 (Lofthus and Krupenie, 1977)

$$E_{vJ} = E_v + B_v J(J+1) - D_v J^2(J+1)^2$$

v	E_v (eV)	B_v (10^{-4}eV)	D_v (10^{-10}eV)
0	0.0	2.4668	7.1
1	0.2888	2.4452	7.132
2	0.5742		
3	0.8559		
4	1.1342	2.3805	
5	1.4088	2.3584	
6	1.6801	2.3365	
7	1.9475		
8	2.2115		
9	2.4718		
10	2.7284	2.2480	
11	2.9815	2.2263	
12	3.2310	2.2033	
13	3.4769	2.1809	
14	3.7191	2.1581	
15	3.9576	2.1354	
16	4.1923		
17	4.4242		
18	4.6510		
19	4.8748		
20	5.0949		
21	5.3114		

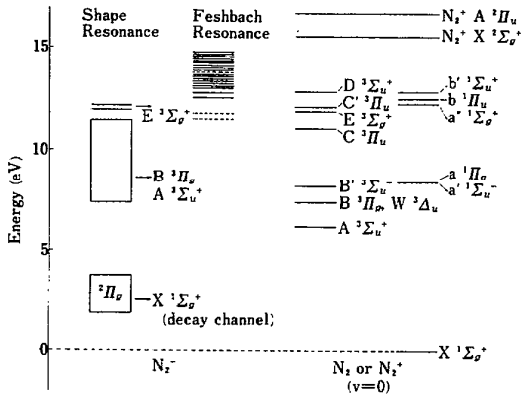

FIG. 2.1. Temporary negative ion states of N_2. Their locations are indicated with respect to the levels of N_2 and N_2^+. The grandparents of the Feshbach resonances are separately denoted by solid (N_2^+ A $^2\Pi_u$) and dashed (N_2^+ X $^2\Sigma_g^+$) lines. (See Refs. 86 and 101.)

2.2. Molecular Properties

Nitrogen has isotopes of mass 14 and 15. Since the natural abundance of the isotope ^{14}N is 99.64%, almost all nitrogen molecules are $^{14}N_2$, the mass of which is

$$M = 4.650\,60 \times 10^{-23}\ \text{g}. \qquad (2.2)$$

This gives the ratio

$$m_e/M = 1.9588 \times 10^{-5}, \qquad (2.3)$$

where m_e is the electron mass.

The nitrogen molecule has an electric quadrupole moment defined by

$$Q = \frac{1}{2}\int \rho(\mathbf{r})(3z^2 - r^2)d\mathbf{r}. \qquad (2.4)$$

Here ρ is the charge distribution (including nuclear charge)

Table 2.5. Matrix elements of quadrupole moment between vibrational states, $\langle v|Q|v'\rangle$. (Cartwright and Dunning, 1974)

	v = 0	1	2	3
v' = 0	-1.669(-26)[a]	5.564(-28)	-3.568(-29)	4.347(-30)
1		-1.657(-26)	7.888(-28)	-6.429(-29)
2			-1.644(-26)	9.680(-28)
3				-1.631(-26)

[a] In units of esu cm^2 (1 esu cm^2 = 3.336 x 10^{-14} C m^2); -1.669(-26) = -1.669 x 10^{-26}.

of the molecule and the z axis is taken along the molecular axis. In 1966, Stogryn and Stogryn[114] surveyed the experimental, as well as theoretical, data on Q and recommended the value

$$Q = -1.52\times10^{-26}\ \text{esu cm}^2 . \tag{2.5}$$

Since then a few measurements were done to obtain Q.[14,21,23] All of their results are consistent with the above value. Birnbaum and Cohen[14] give also the hexadecapole moment,

$$\Phi = \frac{1}{8}\int \rho(\mathbf{r})(35z^4 - 30r^2z^2 + 3r^4)d\mathbf{r}$$
$$= (3\pm1)\times10^{-42}\ \text{esu cm}^4 . \tag{2.6}$$

The dependence of Q on the internuclear distance R was calculated by Cartwright and Dunning[28] and by Morrison and Hay.[84] From their calculation, Cartwright and Dunning obtained the matrix elements of Q between different vibrational states of (nonrotating) N_2. Those for several lowest states are shown in Table 2.5. The quantity $\langle v=0|Q|v'=0\rangle$ corresponds to the quadrupole moment measured. The difference between the theory and the above recommended value is about 10%. Because Stogryn and Stogryn[114] gave no estimate of the uncertainty in their value, it is difficult to determine the reliability of the calculation.

The polarizability of N_2 has two components: $\alpha_\parallel$ and $\alpha_\perp$. The quantity $\alpha_\parallel$ ($\alpha_\perp$) denotes the polarization induced by a field parallel (perpendicular) to the molecular axis. From the distribution of dipole oscillator strengths, Zeiss *et al.*[136] determined the best value of the isotropic part of the polarizability as

$$\alpha_0 = \tfrac{1}{3}(\alpha_\parallel + 2\alpha_\perp)$$
$$= 1.740\times10^{-24}\ \text{cm}^3 . \tag{2.7}$$

The determination of the anisotropy of the polarizability is more difficult than that of α_0. Using the depolarization at the Rayleigh scattering, Alms *et al.*[6] obtained the value

$$\gamma = \alpha_\parallel - \alpha_\perp$$
$$= 0.66\times10^{-24}\ \text{cm}^3 . \tag{2.8}$$

This is about 5% smaller than the old data by Bridge and Buckingham.[19]

From the experiment of vibrational Raman scattering, Buldakov *et al.*[24] derived the derivatives of the polarizability

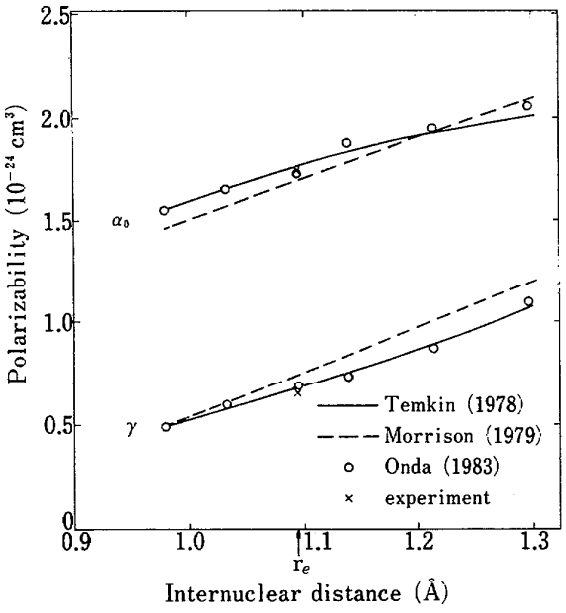

FIG. 2.2. Dependence of the polarizability (isotropic part, α_0 and anisotropic part, γ) on the internuclear distance. Theoretical values are: solid line, Temkin (Ref. 122); dashed line, Morrison and Hay (Ref. 84); circles, Onda and Temkin (Ref. 91). For comparison, experimental data [Eqs. (2.7) and (2.8)] are shown at the equilibrium internuclear distance (r_e).

with respect to the internuclear distance at its equilibrium value (r_e):

$$\left(\frac{d\alpha_0}{dR}\right)_{R=r_e} = 1.72\times10^{-16}\ \text{cm}^2 , \tag{2.9a}$$

$$\left(\frac{d\gamma}{dR}\right)_{R=r_e} = 1.97\times10^{-16}\ \text{cm}^2 . \tag{2.9b}$$

Table 2.6. Vibrational matrix elements of isotropic (α_0) and anisotropic (γ) parts of the dipole polarizability

	v = 0	1	2	3	4
v' = 0	1.768(0)[a,b]	5.029(-2)	-5.597(-3)	5.859(-4)	-4.401(-5)
	6.900(-1)	5.597(-2)	-1.581(-3)	1.974(-5)	3.498(-6)
1		1.775(0)	7.014(-2)	-9.636(-3)	1.186(-3)
		7.055(-1)	7.991(-2)	-2.834(-3)	4.502(-5)
2			1.783(0)	8.469(-2)	-1.354(-2)
			7.214(-1)	9.878(-2)	-4.146(-3)
3				1.790(0)	9.639(-2)
				7.373(-1)	1.151(-1)
4					1.799(0)
					7.535(-1)

[a] The first and second entries are, respectively, $\langle v|\alpha_0|v'\rangle$ and $\langle v|\gamma|v'\rangle$ in units of 10^{-24} cm^3. (6.900(-1)=6.900x10^{-1})

[b] Data are from the unpublished supplement to Onda and Temkin (1983).

In a similar way, Asawaroengchai and Rosenblatt[9] obtained the value of $(d\gamma/dR)_{R=r_e}$ ($= 1.40\times10^{-16}$ cm^2), which is about 30% lower than that of Buldakov *et al.*[24] On the other hand, the calculation by Morrison and Hay[84] gives $(d\gamma/dR)_{R=r_e} = 1.73\times10^{-16}$ cm^2, which lies in between the two measurements. It is uncertain at present which is the best.

There are several calculations reported on the dependence of the polarizability on R. Three of them[84,91,122] are shown in Fig. 2.2. All of the theoretical values are in good agreement. The calculations reproduce the experimental values well for α_0, γ, and $d\alpha_0/dR$ at $R = r_e$. The calculated result of $d\gamma/dR$ at $R = r_e$, however, is somewhat different from the experiment (see above). Onda and Temkin[91] calculated the matrix elements of the polarizability between vibrational states. Those results are shown in Table 2.6.

2.3. Quantities Related to Absorption and Emission of Radiation (Bound–Bound Processes)

a. Wavelengths

Bandhead wavelengths of N_2 and N_2^+ were compiled by Wallace.[127,128] Also the reviews by Lofthus and Krupenie[74] and by Suchard and Melzer[115] contain the lists of the wavelengths of the band origin for various bound–bound transitions in N_2 and N_2^+.

b. Lifetimes and Transition Probabilities

Lifetimes of electronically excited states or transition probabilities for bound–bound processes have been studied extensively. Data compilations were made by Anderson,[7] Suchard and Melzer,[115] Lofthus and Krupenie,[74] and Kuz'menko *et al.*[72]

Table 2.7. Lifetimes (in seconds) of electronic states of N_2
I. Triplet states, calculated by Werner et al. (1984)

v'	$B^3\Pi_g \rightarrow A^3\Sigma_u^+$ $W^3\Delta_u$	$C^3\Pi_u \rightarrow B^3\Pi_g$	$W^3\Delta_u \rightarrow B^3\Pi_g$	$B'^3\Sigma_u^- \rightarrow B^3\Pi_g$
0	13.4(-6)[a]	3.67(-8)	31.6[b]	4.60(-5)
1	11.0(-6)	3.65(-8)	4.52(-3)	3.61(-5)
2	9.31(-6)	3.69(-8)	1.22(-3)	3.01(-5)
3	8.15(-6)	3.77(-8)	6.07(-4)	2.59(-5)
4	7.30(-6)	3.94(-8)	3.80(-4)	2.30(-5)
5	6.65(-6)		2.68(-4)	2.08(-5)
6	6.16(-6)		2.03(-4)	1.90(-5)
7	5.77(-6)		1.62(-4)	1.77(-5)
8	5.46(-6)		1.34(-4)	1.65(-5)
9	5.23(-6)		1.15(-4)	1.56(-5)
10	5.05(-6)		1.00(-4)	1.48(-5)
11	4.92(-6)		8.88(-5)	1.42(-5)
12	4.82(-6)		7.98(-5)	1.36(-5)

[a] 13.4(-6)=13.4x10^{-6}.

[b] Decays also to $X^1\Sigma_g^+$, the lifetime for which is 4 sec (Benesch, 1979).

Table 2.8. Lifetimes (in seconds) of electronic states of N_2 II. The states other than those listed in Table 2.7 (selected from the compilation by Lofthus and Krupenie (1977))

State	Lifetime
$A^3\Sigma_u^+$ (v=0)	1.9
$D^3\Sigma_u^+$ (v=0)	1.41x10^{-8}
$E^3\Sigma_g^+$	1.90x10^{-4}
$a'^1\Sigma_u^-$	0.5
$a^1\Pi_g$	1.15x10^{-4}
$w^1\Delta_u$ (v=0~4)	(1–5)x10^{-4}

Here the lifetimes are summarized separately for each bound–bound transition. Table 2.7 gives the lifetimes of the triplet states of N_2 obtained from a recent calculation by Werner *et al.*[130] They used highly correlated multiconfiguration wave functions and claimed an accuracy of about 10% for the resulting lifetimes. Comparisons to the experimental data or empirical values are made in the original paper. Table 2.8 shows the lifetimes of other states of N_2 taken from Lofthus and Krupenie.[74] The lifetimes of the states of N_2^+ are presented in Table 2.9, which is based on the calculation by Collins *et al.*[35] For the experimental data, see the review by Lofthus and Krupenie.[74]

Tables of the Franck–Condon factors for the bound–bound transitions are given in the reviews by Lofthus and Krupenie[74] and Suchard and Melzer.[115]

c. Distribution of Dipole Oscillator Strengths and its Moments

The distribution of dipole oscillator strengths determines most of the optical properties of the molecule. It is also of significance in understanding the interaction of fast charged particles with molecules.[65] The oscillator strength distribution can be characterized by its moments. In particu-

Table 2.9. Lifetimes (in seconds) of electronic states of N_2^+, calculated by Collins et al. (1980).

v'	$A^2\Pi_u \rightarrow X^2\Sigma_g^+$	$B^2\Sigma_u^+ \rightarrow X^2\Sigma_g^+$	$C^2\Sigma_u^+ \rightarrow X^2\Sigma_g^+$	$D^2\Pi_g \rightarrow B^2\Sigma_u^+$	$D^2\Pi_g \rightarrow A^2\Pi_u$
0	17.45(-6)[a]	5.52(-8)	6.05(-8)	4.25(-4)	2.87(-7)
1	14.76(-6)	5.38(-8)	5.90(-8)	1.62(-4)	2.93(-7)
2	12.90(-6)	5.30(-8)	5.69(-8)	9.42(-5)	2.97(-7)
3	11.54(-6)	5.27(-8)	5.45(-8)	6.65(-5)	3.02(-7)
4	10.50(-6)	5.27(-8)	5.19(-8)	5.29(-5)	3.21(-7)
5	9.69(-6)	5.33(-8)	5.94(-8)	4.57(-5)	3.59(-7)

[a] 17.45(-6)=17.45x10^{-6}.

Table 2.10. Moments of dipole oscillator strengths (Zeiss et al., 1977)

μ	$S(\mu)$	$L(\mu)$	$I(\mu)$ (in eV)
2	4.920(4)[a]	3.414(5)	1.404(4)
1	2.760(2)	1.126(3)	8.045(2)
0	1.400(1)	2.511(1)	8.178(1)
-1/2	7.106		
-1	4.742	3.091	2.611(1)
-3/2	3.599		
-2	2.935	1.039	1.939(1)
-5/2	2.512		
-3	2.226		
-4	1.882		
-6	1.591		
-8	1.502		
-10	1.498		
-12	1.540		
-14	1.615		

[a] 4.920(4)=4.920x10^4.

lar, the following types of moments are useful:

$$S(\mu) = \sum_n \left(\frac{E_n}{\mathrm{Ry}}\right)^\mu f_n + \int_{I_1}^\infty \left(\frac{E}{\mathrm{Ry}}\right)^\mu \frac{df}{dE}\,dE\,, \quad (2.10)$$

$$L(\mu) = \sum_n \left(\frac{E_n}{\mathrm{Ry}}\right)^\mu \ln\left(\frac{E_n}{\mathrm{Ry}}\right) f_n + \int_{I_1}^\infty \left(\frac{E}{\mathrm{Ry}}\right)^\mu \ln\left(\frac{E}{\mathrm{Ry}}\right) \frac{df}{dE}\,dE\,, \quad (2.11)$$

$$I(\mu) = \exp[L(\mu)/S(\mu)]\mathrm{Ry}\,. \quad (2.12)$$

Here E_n is the excitation energy of the nth state, f_n is the dipole oscillator strength for the excitation from the ground to the nth state, df/dE is the density of the oscillator strength per unit energy for continuum excitation, and I_1 is the first ionization potential. All the energies are expressed in rydberg units (1 Ry = 13.61 eV).

From the thorough investigation of the experimental and theoretical data on photoabsorption and electron collisions, Zeiss *et al.*[136] determined semiempirically the best values of the above moments. Those are listed in Table 2.10. (Note that the definition of the moment by Zeiss *et al.*[136] is different from the one above. The values in Table 2.10 have been adjusted to the present definition.) Very recently, Kosman and Wallace[71] made a complete calculation of the distribution of dipole oscillator strengths and analyzed them by decomposing to the contributions from various subshells and several wavelength ranges.

3. Photoionization and Photodissociation

3.1. Photoionization

A number of measurements have been reported on the photoionization or photoabsorption of nitrogen molecules. In 1979, Berkowitz[11] and Kirby *et al.*[70] independently published their recommended data based on an extensive survey of the literature. In the present paper, recommended values of the photoionization cross section are redetermined with some recent results taken into account. The final values are very similar to the previous recommended data.

a. Total Cross Section

Samson *et al.*[99] measured the absolute absorption cross section and the photoionization yield (the ratio of the photoionization to the photoabsorption cross sections) using a double ionization chamber and a line radiation source, over the wavelength range from 800 to 100 Å. They claimed an accuracy of 3% for their photoionization cross sections. Their data are in quite good (within 1%) agreement with those obtained by Wight *et al.*[132] with the use of electron-impact technique. In the region of shorter wavelengths (< 550 Å), several measurements of photoabsorption cross section were done (de Reilhac and Damany,[45] for 500–100 Å; Cole and Dexter,[34] for 340–50 Å; Denne,[44] for 82–24 Å). In this energy range, the ionization yield has been confirmed to be unity so that the photoabsorption cross section is equivalent to the photoionization cross section.

For the wavelengths of 650–50 Å the five sets of data described above coincide with each other within the com-

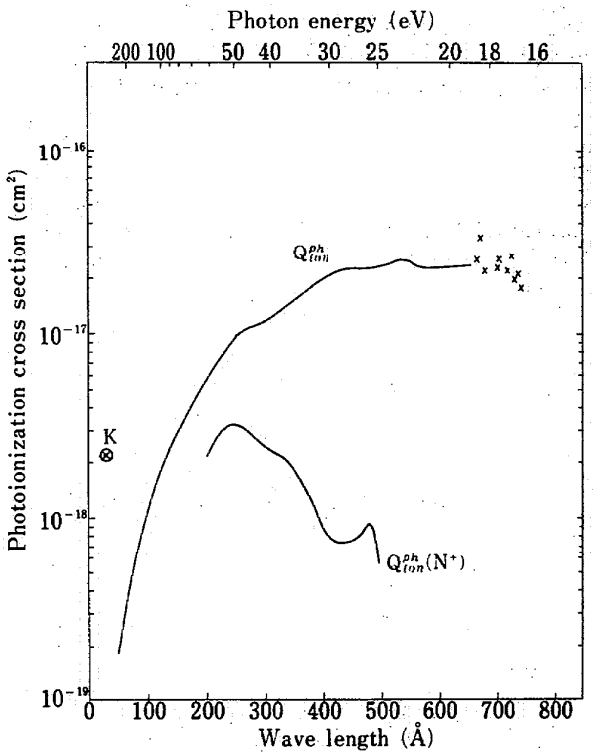

FIG. 3.1. Total (Q^{ph}_{ion}) and dissociative [$Q^{ph}_{ion}(N^+)$] photoionization cross sections. In the region of the wavelengths longer than 650 Å, only the representative data are shown. More details for the region are presented in Figs. 3.2a and 3.2b. The peak cross section at the K-absorption shape resonance is indicated by the letter K.

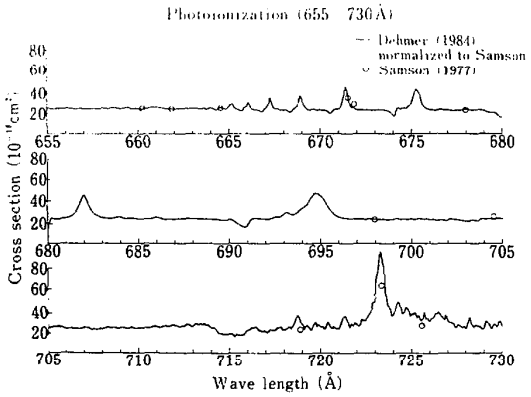

FIG. 3.2a. Photoionization cross section at wavelengths 655–730 Å. The relative values measured by Dehmer *et al.* (Ref. 43) are normalized to the data by Samson *et al.* (Ref. 99) in the region 660–665 Å.

bined errors of the measurements. The best values of the photoionization cross section have been determined by smoothly connecting the midpoints of those data. The result is shown in Fig. 3.1. The overall accuracy of the present cross section is about 10%, but the longer wavelength region (> 300 Å) should be more accurate (probably 3%–5%). Below about 31 Å, a strong *K*-absorption occurs.[13] The maximum value of the shape-resonance part of the *K*-absorption cross section is also shown in Fig. 3.1. Bianconi *et al.*[13] further found a very sharp peak (1.74×10^{-17} cm^2 at 30.9 Å) due to the *K*-absorption just below the shape resonance.

Between 650 and 800 Å, there are many discrete absorptions followed by autoionization. Dehmer *et al.*[43] detected N_2^+ on the impact of light in this wavelength range. They reported the yield of N_2^+ in a relative scale. Here we have normalized their relative photoionization cross section to those measured by Samson *et al.*[99] over the wavelength region of 660–665 Å. The result is shown in Figs. 3.2a and 3.2b, together with Samson's data. The wavelength resolution of the original data of Dehmer *et al.* is 0.023 Å in the region from 797 to 712 Å and 0.069 Å otherwise. In Figs. 3.2a and 3.2b, the original values are plotted every 0.1 Å. The very fine structure, therefore, is not reproduced there.

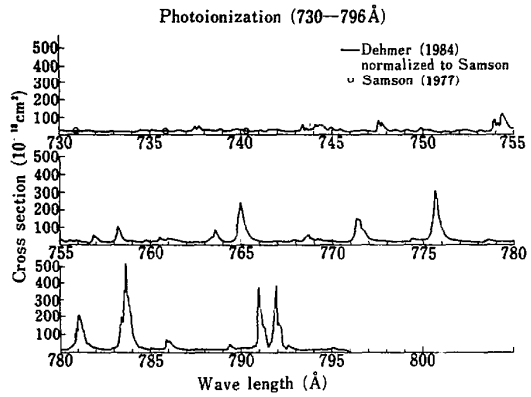

FIG. 3.2b. Photoionization cross section at wavelengths 730–796 Å. The relative values measured by Dehmer *et al.* (Ref. 43) are normalized to the data by Samson *et al.* (Ref. 99) in the region 660–665 Å.

Cole and Dexter[34] estimated the contribution of $N_2^{+\,+}$ to the ionization cross section. They concluded that the fraction of $N_2^{+\,+}$ in the total yield of ions is around 6%–7% at 180–210 Å and decreases to about 2% at the wavelength longer than 260 Å. This is consistent with another estimate by Wight *et al.*[132]

b. Partial Cross Sections

Samson *et al.*[99] reported also the partial photoionization cross sections for the production of N_2^+ in its states $X\,^2\Sigma_g^+$, $A\,^2\Pi_u$, and $B\,^2\Sigma_u^+$. They obtained the cross sections from the branching ratios measured by the photoelectron spectroscopy technique and normalized to their own total photoionization cross section. Hamnett *et al.*[56] also obtained the branching ratios by the (e,2e) coincidence method. Normalizing the data to the total cross section of Wight *et al.*,[132] they reported the partial cross sections. Those two sets of partial cross sections are in general agreement. A smoothed curve drawn through the data points of the two sets is shown in Fig. 3.3.

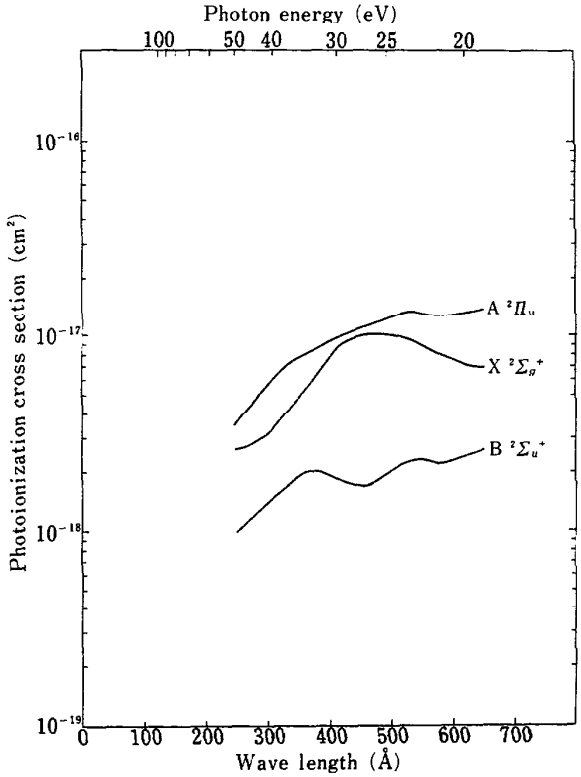

FIG. 3.3. Partial photoionization cross sections for the production of N_2^+ in the states $X\,^2\Sigma_g^+$, $A\,^2\Pi_u$, $B\,^2\Sigma_u^+$.

c. Dissociative Ionization

Wight *et al.*[132] measured the cross section for the production of N^+ using the electron–ion coincidence technique. Their values are plotted in Fig. 3.1. Recently, Morioka *et al.*[83] measured the yield of N^+ with the use of the synchrotron radiation over the wavelengths from the threshold (510.2 Å) to 450 Å. Their cross section near the threshold has a rich structure due to autoionization. Absolute magnitudes of the cross section are by about a factor of 2 larger than the result of Wight *et al.*[132] It is hard to clarify the discrepancy because of the complete difference between the two methods of measurement.

3.2. Photodissociation

At the wavelengths shorter than 1270 Å, photons can dissociate N_2 to two nitrogen atoms. Though there are several papers (e.g., Ref. 36) discussing this process, no definite conclusion has been obtained about the magnitude of the cross section.

Above the ionization threshold, ionization yield η can give information about the contribution of the dissociation process. In this region, photoabsorption results in either ionization or dissociation. Thus we have

$$\eta = \frac{Q^{\rm ph}_{\rm ion}}{Q^{\rm ph}_{\rm ion} + Q^{\rm ph}_{\rm diss}} . \tag{3.1}$$

From this relation, the photodissociation cross section $Q^{\rm ph}_{\rm diss}$ can be estimated, once η and the photoionization cross section $Q^{\rm ph}_{\rm ion}$ are known. Samson *et al.*[99] concluded from their experiment that η is unity for the wavelengths shorter than 660 Å and varies between 76% and 97% in the region 660–740 Å. Carter and Berkowitz[27] reported η of an average value of 85% in the wavelength region 734–796 Å. When we consider the possibility of predissociation, $Q^{\rm ph}_{\rm diss}$ would be very much dependent on the wavelength. The direct measurement of $Q^{\rm ph}_{\rm diss}$ with a high-wavelength resolution is desirable.

Below the ionization threshold, a detailed absorption spectrum can give information on $Q^{\rm ph}_{\rm diss}$. The absorption cross sections obtained by Gürtler *et al.*,[54] for example, show significant continuum absorption in the region 810–840 Å. This may be attributed to the dissociation process. Band absorption, however, may contribute also to the dissociation through predissociation process.

3.3. References for Further Details of Photoionization

Angular distribution of photoelectrons was measured for each of the ionic states, $X\,^2\Sigma_g^+$, $A\,^2\Pi_u$, $B\,^2\Sigma_u^+$ over the wavelength from 620 to 276 Å.[77] The dependence of the photoionization cross section on the vibrational states of the ion was measured several times (e.g., Gardner and Samson[52]). The result is approximately reproduced by the Franck–Condon factors between the initial and the final vibrational states. When a resonance occurs, however, the Franck–Condon factor approximation fails.[131] The vibrational dependence of the angular distribution was also studied.[26,61]

4. Electron Collisions: Total-Scattering, Elastic, and Transport Cross Sections

4.1. Total-Scattering Cross Sections

In 1981, Hayashi[57] surveyed the data available and determined the best values of the total-scattering cross section Q_T. His data were based mostly on the results by Blaauw *et al.*,[15] Kennerly,[69] and Dalba *et al.*[40] Since then three new measurements have been reported.[59,66,87] Taking into account those recent results, we have slightly modified Hayashi's Q_T. The resulting values are shown in Figs. 4.1 and 4.2. On the consideration of the high accuracy of the original data, the uncertainty in the present Q_T is $\pm$ 5%.

4.2. Elastic Scattering and Transport Cross Sections

In his paper, Hayashi[57] determined the best value also for the elastic cross section $Q_{\rm elas}$, the momentum-transfer cross section $Q_{\rm m}$, and the viscosity cross section $Q_{\rm vis}$. The latter two are called the transport cross sections and defined by

$$Q_{\rm m}(E) = 2\pi \int_0^\pi d\theta q(E,\theta)(1-\cos\theta)\sin\theta , \tag{4.1}$$

$$Q_{\rm vis}(E) = 2\pi \int_0^\pi d\theta q(E,\theta)(1-\cos^2\theta)\sin\theta , \tag{4.2}$$

where $q(E,\theta)$ is the elastic differential cross section at the electron energy E and the scattering angle θ. Hayashi evaluated the cross sections using the data on $q(E,\theta)$ obtained by beam measurements.[20,29,47,108,111]

Here we have revised Hayashi's values by taking account of the new results of the total scattering cross section (Sec. 4.1) and the vibrational cross section (Sec. 6), as described below. The resulting values of $Q_{\rm elas}$, $Q_{\rm m}$, and $Q_{\rm vis}$ are shown in Figs. 4.1 and 4.2.

For the electron energies larger than 4 eV, the elastic cross section of Hayashi[57] has been modified slightly to be consistent with the present value of Q_T. In the region from 1

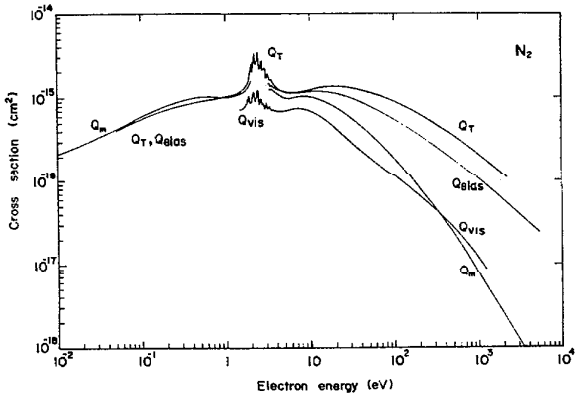

FIG. 4.1. Total scattering (Q_T), elastic ($Q_{\rm elas}$), momentum-transfer ($Q_{\rm m}$), and viscosity ($Q_{\rm vis}$) cross sections. Details around the 2.3 eV shape resonance are shown in Fig. 4.2.

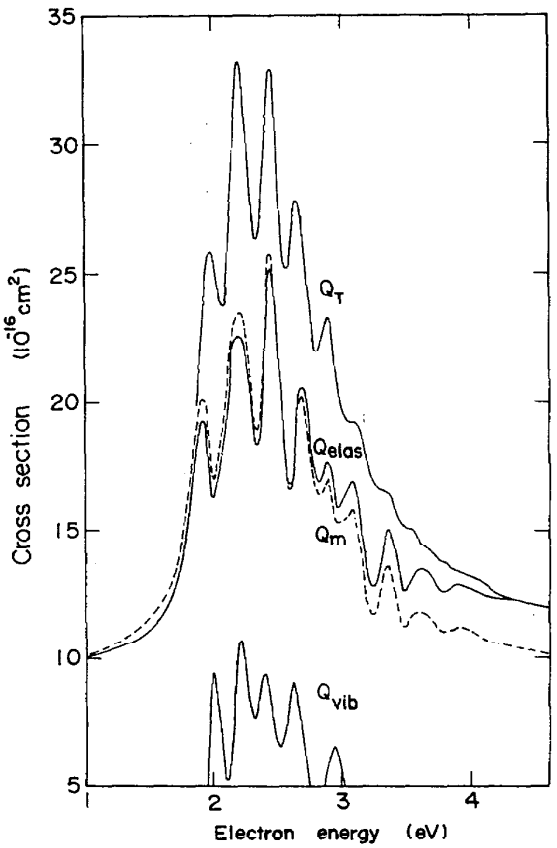

FIG. 4.2. Details of the total scattering (Q_T), elastic (Q_{elas}), and momentum-transfer (Q_m) cross sections in the region of the 2.3 eV shape resonance. Sum of the vibrational cross sections, $Q_{vib} = \Sigma_{v'=1}^{9} Q_{vib}$ ($v = 0 \rightarrow v'$) is also shown for comparison.

to 4 eV, the resonance structure has been considered in the following manner. No excitation to the electronic excited states can occur in this energy region. The best values of the vibrational excitation cross section are determined in Sec. 6 on the basis of the most recent calculation of Onda and Temkin.[92] Then the elastic cross section has been obtained from the relation

$$Q_{elas}(E) = Q_T(E) - \sum_{v'=1} Q_{vib} \quad (v = 0 \rightarrow v'; E) . \quad (4.3)$$

Experimental data on Q_{elas} are available at several energies in this region.[67,108] The present Q_{elas} agrees with them within about 30%. On the consideration of the difficulty of beam measurement in this resonance region, this agreement is quite satisfactory.

The transport cross sections at 1–4 eV have been calculated simply by the formulas

$$Q_m(E) = C_m Q_{elas}(E) , \quad (4.4)$$

$$Q_{vis}(E) = C_{vis} Q_{elas}(E) . \quad (4.5)$$

The constants C_m and C_{vis} have been taken to be an average of the ratios Q_m/Q_{elas} and Q_{vis}/Q_{elas} obtained from the experimental data on the differential cross sections by Shyn and Carignan[108] in this energy range. Actually the experimental ratios do not change much there.

At the electron energies less than 1 eV, Q_{elas} can be set equal to Q_T and use has been made of the Q_m determined by swarm analysis.[49]

Finally it should be noted that the elastic cross section here includes the effect of rotational transitions (see Sec. 5.3). In this sense, the present elastic cross section should be called "vibrationally elastic."

5. Electron Collisions: Rotational Transitions

5.1. Rotational Transitions from the Ground State ($J = 0$)

Because of the very narrow level spacings, it is difficult to measure the rotational excitation cross section by the beam method, although a few such measurements have been performed and the results of those are mentioned below. On the other hand, a large number of theoretical studies have been made on the rotational transitions in N_2 (see, e.g., Ref. 73). The reliability of the calculations varies and the resulting cross sections scatter by more than a factor of 2.[116] Here we give no detailed survey of the theoretical studies, but show the cross sections selected from several recent works.

a. $E < 3$ eV

Very recently, Onda[90] made an elaborate calculation of the rotational transitions taking into account target polarization and electron exchange, both of which are very important in low-energy electron molecule collisions. His calculation is based on the assumption of fixed nuclei except in the resonance region (2–3 eV), in which the vibrational motion is considered correctly.

Figure 5.1 shows Onda's results for the rotational excitations $J = 0 \rightarrow 2,4,6,8$. (Because of the molecular symmetry, rotational transitions with $\Delta J =$ odd are forbidden.) The details of the cross sections for $0 \rightarrow 2$ and 4 in the resonance region are shown separately in Fig. 5.2. There are sev-

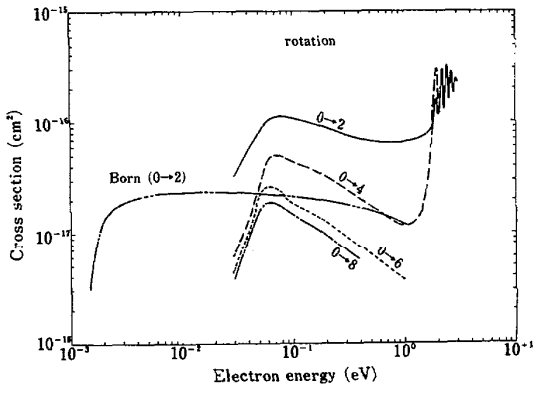

FIG. 5.1. Cross sections for the rotational excitations $J = 0 \rightarrow 2,4,6,8$. All the cross sections but for the Born ($0 \rightarrow 2$) value are calculated by Onda (Ref. 90). The Born cross section is evaluated with the quadrupole and polarization interactions taken considered.

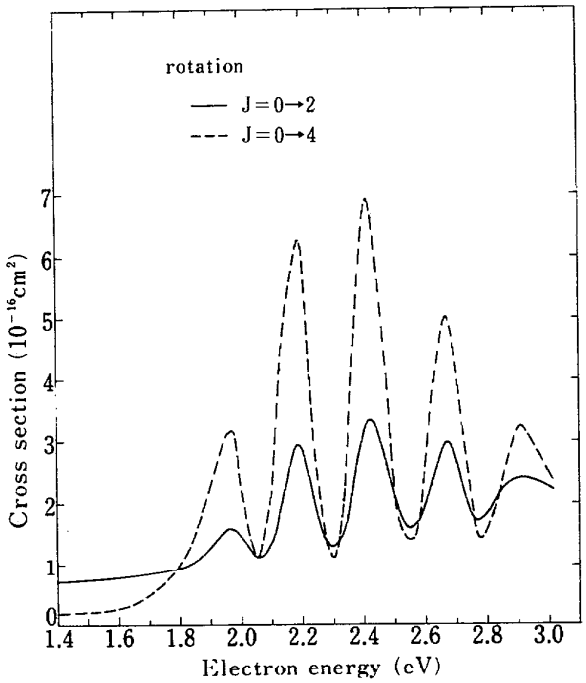

FIG. 5.2. Details of the rotational cross sections for $J = 0 \rightarrow 2,4$ calculated by Onda (Ref. 90) in the region of the shape resonance.

eral characteristic features to be noted. First, in the resonance region, the transition $0 \rightarrow 4$ occurs much more frequently than $0 \rightarrow 2$. This has already been pointed out by many authors (e.g., Chandra and Temkin,[31] Buckley and Burke[22]). The transitions $0 \rightarrow J$ with $J > 4$ have a small cross section (about two orders of magnitude less than that for $0 \rightarrow 2$). Also a significant enhancement of the cross section occurs around the electron energy of 0.07 eV. The physical meaning of this is to be studied.

Near the threshold the Born approximation can give fairly reliable results for the $0 \rightarrow 2$ transition, when the quadrupole and polarization interactions are properly taken into account. Figure 5.1 shows the Born cross section calculated with the formula of Dalgarno and Moffett[41] and the molecular parameters used in Onda's calculation. Probably the true cross section would go smoothly from the Born value at the lower energy to the result of the more elaborate calculation at the higher energy.

In this energy region, two beam-type measurements were done.[67,134] To analyze the electron energy-loss spectra, both of them employed the high-J approximation. Their result is a kind of cross section averaged over the rotational population of N_2. This makes it difficult to compare those experimental data directly to the present theoretical values.

b. $E > 3$ eV

In Table 5.1, the results of two recent calculations[93,94,98] are shown. Also given are the preliminary results of the beam measurement by Tanaka *et al.*[118] All three sets of the cross sections in Table 5.1 are in good agreement. Although we need more definite experimental data, the general trend of the rotational cross section in this energy range can be discerned from the table.

Table 5.1. Rotational excitation cross section (in 10^{-16} cm^2) at higher energies

	Onda[a]			Rumble[b]			experiment[c]	
E(eV)	0→2	0→4	0→6	0→2	0→4	0→6	0→2	0→4
5				3.08	1.57		3.9	1.1
10	3.86	1.35	0.007	3.84	0.99		4.4	0.8
20	3.36	0.80	0.048	3.53	0.86	0.119	2.8	0.8
30	2.86	1.10	0.342	2.77	1.39	0.389		
50	1.63	1.36	0.278	1.64	1.41	0.241		

[a] Onda and Truhlar (1979,1980).

[b] Rumble et al. (1983).

[c] Tanaka et al. (1980).

5.2. Rotational Transitions from Excited States ($J \neq 0$)

Under the adiabatic-rotation approximation, the cross section for any rotational transition $J_i \rightarrow J_f$ can be related to those for the transitions from the ground state ($J = 0$).[105] That is, we have

$$Q_{\text{rot}}(J_i \rightarrow J_f) = \sum_J [C(J_i J J_f; 000)]^2 Q_{\text{rot}}(0 \rightarrow J) , \quad (5.1)$$

where $C(J_i J J_f; 000)$ is the Clebsch–Gordan coefficient. This relation can be used unless the electron energy is in the near vicinity of the threshold (for more details, see Shimamura's article in Ref. 106).

5.3. Remarks on the Elastic Cross Section

When a beam method is applied to experimentally obtain the elastic cross section for N_2, it is very difficult to resolve the effect of the rotational transitions accompanied. Thus the following average cross sections are of practical use:

(1) rotationally-inelastic cross section,

$$\bar{Q}_{\text{rot}}(E, T_{N_2}) = \sum_J f_J(T_{N_2}) \sum_{J'(\neq J)} Q_{\text{rot}}(J \rightarrow J') , \quad (5.2)$$

(2) rotationally-averaged elastic cross section,

$$\bar{Q}_{\text{elas}}(E, T_{N_2}) = \sum_J f_J(T_{N_2}) Q_{\text{rot}}(J \rightarrow J) , \quad (5.3)$$

(3) vibrationally-elastic cross section,

$$\bar{Q}_{\text{vib-elas}}(E, T_{N_2}) = \sum_J f_J(T_{N_2}) \sum_{J'} Q_{\text{rot}}(J \rightarrow J') ,$$
$$= \bar{Q}_{\text{elas}} + \bar{Q}_{\text{rot}} . \quad (5.4)$$

Here T_{N_2} is the temperature of nitrogen gas and $f_J(T_{N_2})$ is the fractional population of the rotational states of N_2 at the temperature.

Usually a beam measurement gives $\bar{Q}_{\text{vib-elas}}$ as an elastic cross section. The elastic cross sections shown in Sec. 4.2 should be regarded as $\bar{Q}_{\text{vib-elas}}$. When the probability of rotational transition is very low compared with that of the purely elastic collision, i.e.,

$$Q_{\text{rot}}(\Delta J=0) \gg Q_{\text{rot}}(\Delta J \neq 0)\,, \tag{5.5}$$

we have

$$\bar{Q}_{\text{vib-elas}} \simeq \bar{Q}_{\text{elas}}\,. \tag{5.6}$$

In many cases of nonpolar molecules, the relation (5.5) holds. When the electron energy is much higher than the gas temperature, the adiabatic approximation described in the last subsection leads to

$$\bar{Q}_{\text{vib-elas}} = \sum_J Q_{\text{rot}}(0 \rightarrow J) \tag{5.7}$$

and the resulting $\bar{Q}_{\text{vib-elas}}$ does not depend on T_{N_2}. Furthermore, if the condition

$$Q_{\text{rot}}(0 \rightarrow 0) \gg Q_{\text{rot}}(0 \rightarrow J \neq 0) \tag{5.8}$$

holds, we have

$$\bar{Q}_{\text{vib-elas}} \simeq Q_{\text{rot}}(0 \rightarrow 0)\,. \tag{5.9}$$

That is, when the electron energy is much higher than the gas temperature and the rotationally inelastic collision occurs much less frequently than the rotationally elastic one, the measured elastic cross section can be approximately regarded as the purely elastic cross section for the molecule in its rotational ground state. All the beam-type measurements of elastic cross section for N_2 have been carried out so far under such conditions.

6. Electron Collisions: Vibrational Excitations

6.1. Vibrational Excitation: $v = 0 \rightarrow 1$

a. $E < 1.8$ eV

In this region of electron energy, experimental data are available from the swarm analysis done by Engelhardt *et al.*[49] The data are shown in Fig. 6.1. Very recently, Allan[5] made a beam experiment using a trochoidal electron spectrometer. His method gives only the differential cross section at the scattering angles of 0° and 180°. From the values he crudely estimated the integrated cross section, which agrees well with the swarm data. More direct measurement of the integral cross section is still needed.

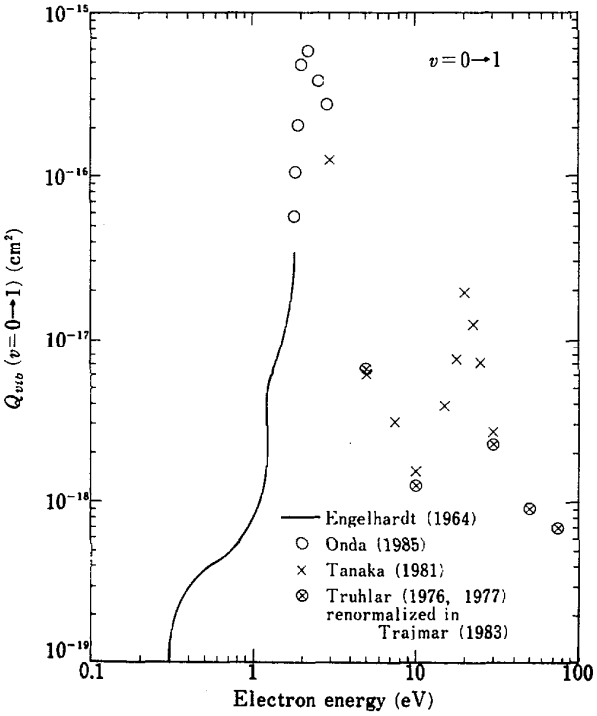

FIG. 6.1. Cross sections for the vibrational excitation, $v = 0 \rightarrow 1$. Only representative values are shown for the theoretical result of Onda and Temkin (Ref. 92), details of which are presented in Fig. 6.2. Experimental data are from beam measurements by Tanaka *et al.* (Ref. 119) and Truhlar *et al.* (Refs. 125 and 126) (renormalized in Trajmar *et al.*, Ref. 124), and from swarm analysis by Engelhardt *et al.* (Ref. 49).

b. 1.8 eV $< E <$ 3 eV

This is the region where a shape resonance has a very large effect on the vibrational cross section. There are several measurements of the cross section, but most of them give the differential cross section at only a few scattering angles. The absolute magnitude of the integrated cross section still remains uncertain. Also a large number of calculations have been done for this process, but the results differ widely depending on the methods used (see the review articles mentioned in Sec. 1).

Here we adopt the most recent calculation by Onda and Temkin.[92] They take into account the effects of electron exchange and target polarization, especially the dependence of the effects on the internuclear distance. The rotational states are taken to be adiabatic, but the coupling among vibrational states is considered correctly. Furthermore, they solve a set of partial-differential coupled equations to avoid inaccuracy arising from the conventional method of partial-wave expansion.

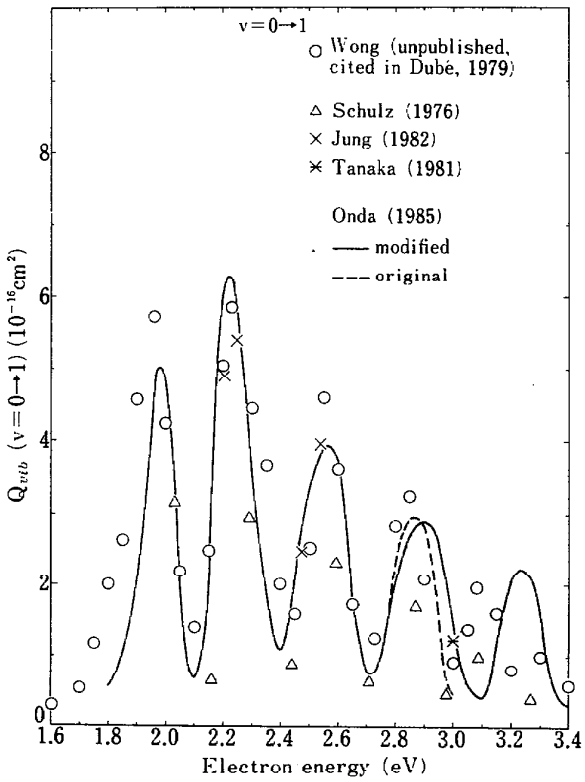

FIG. 6.2. Details of the vibrational excitation cross section for $v = 0 \rightarrow 1$ in the region of the shape resonance. Theoretical results of Onda and Temkin (Ref. 92) are compared with measurements (Refs. 67, 102, 119, and Wong, unpublished but cited in Ref. 46). Only the maximum and minimum values for each peak are shown for Schulz's data (Ref. 102). The original values of Onda and Temkin (Ref. 92) have been modified and extended in the higher energy region (see text).

The cross sections of Onda and Temkin[92] are in fairly good agreement with the unpublished experimental data by Wong (cited in Ref. 46) and the recent measurement by Jung *et al.*[67] (see Fig. 6.2). The total scattering cross section $[Q_T = Q_{elas} + \Sigma_{v'=1} Q_{vib}(0 \rightarrow v')]$ calculated by Onda and Temkin agrees well with the measured value of Q_T. This implies that their calculation is more reliable than most of the other theoretical calculations which cannot or do not produce accurate results for elastic cross section. The cross section obtained by Onda and Temkin for $v = 0 \rightarrow 1$ has a maximum value of about 6×10^{-16} cm^2. This is by about a factor of 2 larger than the result of the measurement by Schulz.[102] Very recently Haddad[55] analyzed the data on the drift velocity of electrons in a mixture of Ar and N_2 and concluded that the vibrational cross section of Schulz is too low. Thus the swarm analysis of Haddad results in the cross section consistent with Wong's unpublished value and hence supports the value of Q_{vib} of Onda and Temkin. A measurement of the absolute cross section by a beam method would be helpful to confirm the present conclusion.

The calculation by Onda and Temkin adjusted one parameter to give a good value of the peak position of the lowest energy. The result of the calculation, therefore, becomes less reliable with increasing energy. Because of this they reported their results only up to 3 eV. To obtain a comprehensive set of cross sections, we need to extend the present vibrational cross section to higher energies. To have values consistent with the Q_T in Fig. 4.1, we modify and extend the original result of Onda and Temkin as shown in Fig. 6.2. In so doing an account has been taken of another recent calculation.[135] The resulting vibrational cross sections are in less agreement with the experimental data than the original ones, but more consistent with the Q_T, whose accuracy is much higher than that for the measurement of Q_{vib}. The modified cross section, together with Q_T, has been used to derive the elastic cross section shown in Fig. 4.2 (see Sec. 4.2).

c. $E > 3$ eV

Two sets of beam data are available.[119,125,126] They are shown in Fig. 6.1. The mutual agreement of the two sets of data is good. For a comparison, two sets of calculations[25,98] are presented in Table 6.1. The absolute magnitude of the cross section at the 20 eV resonance is well reproduced, but the peak position is different from the experiment.

Table 6.1. Vibrational cross sections (in 10^{-16} cm^2) calculated at higher energies

	v = 0 → 1		v = 0 → 2	
E(eV)	Rumble[a]	Burke[b]	Rumble[a]	Burke[b]
5	0.20		0.025	
10	0.020		0.00053	
20	0.076	0.032	0.0023	0.011
25		0.113		0.015
30	0.11	0.076	0.015	0.010
50	0.023		0.00062	

[a] Rumble et al. (1983).

[b] Burke et al. (1983).

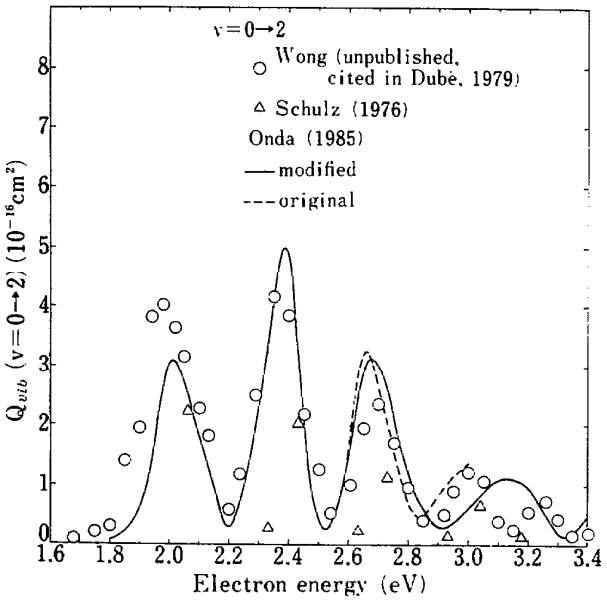

FIG. 6.3. Same as Fig. 6.2, but for the vibrational excitation $v = 0 \rightarrow 2$.

6.2. Other Vibrational Excitations

Onda and Temkin[92] also calculated the vibrational cross sections for $v = 0 \rightarrow v'$ with $v' = 2$–9. Their result for $v = 0 \rightarrow 2$ is shown in Fig. 6.3. As in the case of $v = 0 \rightarrow 1$, their values are in good agreement with Wong's unpublished data and much larger than the old Schulz values. As has been mentioned before, their summed cross section, $\Sigma_{v'=0} Q_{vib}(0 \rightarrow v')$, agrees well with the measured value of Q_T. The cross section for $v = 0 \rightarrow 2$ obtained by Onda and Temkin is also modified, as shown in Fig. 6.3, to be extended to higher energies.

Above the region of the shape resonance, no measurement has been done of the excitation to the higher vibrational states. To enable an estimate, two sets of the calculated results for $v = 0 \rightarrow 2$ are shown in Table 6.1. Aside from the shift of the resonance peak around 20 eV, the two sets of data are in reasonable agreement.

In the present paper, we restrict our discussion to the transition from the ground vibrational state ($v = 0$). A number of theoretical papers provide information on the transitions among excited vibrational states.[12,31,46]

7. Electron Collisions: Electronic Excitations (Nondissociative)

The excitation of electronic states of N_2 has been most frequently studied by the measurement of emission cross section (Q_{emis}). That is, the intensity of radiation emitted is measured at the impact of electrons. The absolute value of Q_{emis} is, however, very difficult to obtain, because of a number of problems (e.g., lack of calibration techniques at shorter wavelengths, radiation trapping, effects of secondary electrons, anisotropy of emitted light, etc. See the recent review by McConkey[78]). Furthermore emission cross section includes the contribution of cascade excitation via higher excited states. Usually it is hard to separate the cascade effects from the direct excitation.

In 1977, the JPL group[29,30,33] published their result of the excitation cross section determined by the measurement of electron energy-loss spectra (ELS). Those data have been recently renormalized because of a significant improvement of the elastic cross section at which the ELS has been normalized.[124] We take these renormalized data as standard here. It should be noted that the renormalization changes the cross section little in the energy region of 15–20 eV, but by up to a factor of 2 in the higher or lower energy region. Considering the accuracy claimed by the original authors, the present renormalized values have uncertainty of 20%–25%.

Table 7.1. List of the cross sections for the electronic excitation of N_2, presented in the figures and tables. Related emission cross sections are also indicated.

State	Q_{exc}	Q_{emis}
$A\ ^3\Sigma_u^+$	Fig. 7.1	
$B\ ^3\Pi_g$	Fig. 7.1	Fig. 7.2 (B → A)
$W\ ^3\Delta_u$	Fig. 7.1	
$B'\ ^3\Sigma_u^-$	Fig. 7.12	
$a'\ ^1\Sigma_u^-$	Fig. 7.12	
$a\ ^1\Pi_g$	Fig. 7.4	Fig. 7.3 (a → X)
$w\ ^1\Delta_u$	Fig. 7.12	
$C\ ^3\Pi_u$	Fig. 7.6	Fig. 7.5 (C → B)
$E\ ^3\Sigma_g^+$	Fig. 7.7	
$a''\ ^1\Sigma_g^+$	Fig. 7.7	
$b\ ^1\Pi_u$	Fig. 7.9	Fig. 7.8 (b → X)
$c'\ ^1\Sigma_u^+$ $(c_4'\ ^1\Sigma_u^+)^a$	Fig. 7.11	Fig. 7.10 (c' → X)
$F\ ^3\Pi_u$ $(\ -\ )^b$	Table 7.2	
$G\ ^3\Pi_u$ $(\ -\ )^b$		
$b'\ ^1\Sigma_u^+$		
$c\ ^1\Pi_u$ $(c_3\ ^1\Pi_u)^a$		
$o\ ^1\Pi_u$ $(o_3\ ^1\Pi_u)^a$		

[a] Corresponding state in Table 2.1.

[b] Listed not in Table 2.1 but in Table 2.2.

We can derive an excitation cross section Q_{exc} from Q_{emis} for a particular line, on the assumption that the cascade contribution can be neglected. (The relation between Q_{exc} and Q_{emis} is given, for instance, in the Appendix of the paper by Aarts and de Heer.[2]) In some cases [see the cases (1) and (2) below], it is apparent that the cascade effects cannot be ignored. For such cases no Q_{exc} is derived from Q_{emis}. Furthermore the Franck–Condon factor approximation is employed here for the electron-impact excitation of associated vibrational levels. In the following, the excitation cross sections thus derived are compared with those obtained from the ELS measurement.

A list of excitation cross sections reported here is given in Table 7.1, where the related emission cross sections are also indicated. There are a number of theoretical calculations of Q_{exc} for N_2. In a recent review, Trajmar and Cartwright[123] made a rather extensive comparison of the theoretical and experimental cross sections. Though progress has been achieved recently, theory is still insufficient to produce reliable cross sections for electronic excitation of molecules. No theoretical values, therefore, will be shown in this report.

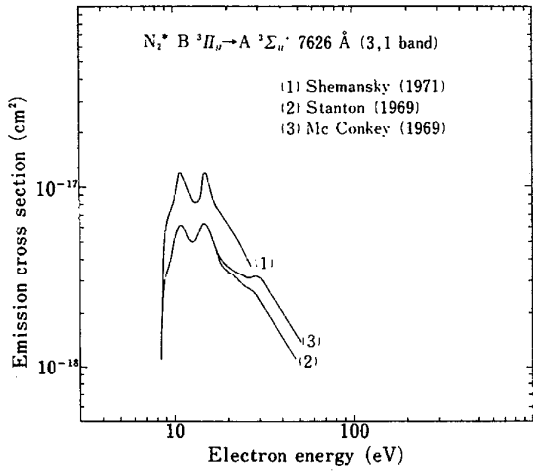

FIG. 7.2. Emission cross sections for the 7626 Å line in the first positive system ($B\,^3\Pi_g \rightarrow A\,^3\Sigma_u^+$) of N_2, measured by (1) Shemansky and Broadfoot (Ref. 104), (2) Stanton and St. John (Ref. 112), and (3) McConkey and Simpson (Ref. 79).

(1) $A\,^3\Sigma_u^+$

The excitation cross section obtained by Cartwright *et al.*[30] is shown in Fig. 7.1. Borst[16] measured the cross section for the production of metastable molecules with a surface detector. The Borst cross section contains a cascade contribution. In this case cascade transitions from $B\,^3\Pi_g$ and other higher states are expected to be very large. No effort, therefore, has been made to derive the direct-excitation part from the Borst data.

(2) $B\,^3\Pi_g$

The emission cross sections[79,104,112] for the 7626 Å line in the transition $B\,^3\Pi_g$–$A\,^3\Sigma_u^+$ (first positive system) are shown in Fig. 7.2. The second peak around 15 eV is probably due to the cascade from the $C\,^3\Pi_u$ state. It is difficult to derive a reliable excitation cross section from these Q_{emis}. The excitation cross section determined from the ELS measurement[30] is shown in Fig. 7.1.

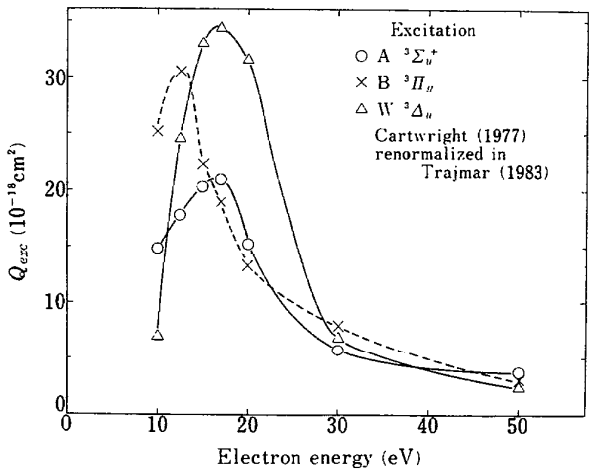

FIG. 7.1 Cross sections for the electronic excitations from the ground state to $A\,^3\Sigma_u^+$, $B\,^3\Pi_g$, and $W\,^3\Delta_u$, measured by Cartwright *et al.* (Ref. 30) and renormalized by Trajmar *et al.* (Ref. 124). Curves are drawn only for guiding eyes.

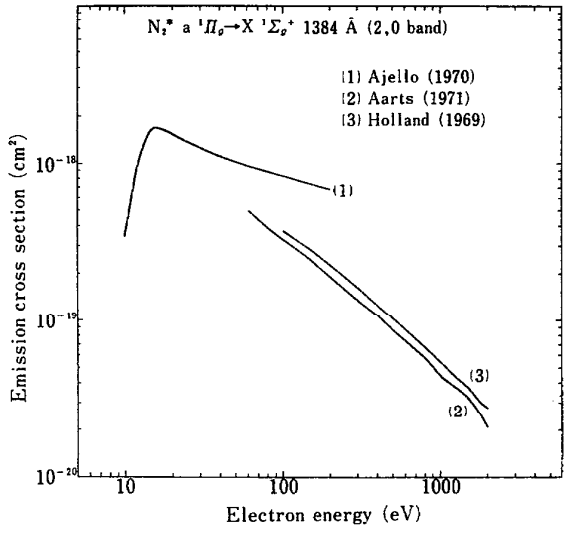

FIG. 7.3. Emission cross sections for the 1384 Å line in the Lyman–Birge–Hopfield system ($a\,^1\Pi_g \rightarrow X\,^1\Sigma_g^+$) of N_2, measured by (1) Ajello (Ref. 4), (2) Aarts and de Heer (Ref. 2), and (3) Holland (Ref. 60).

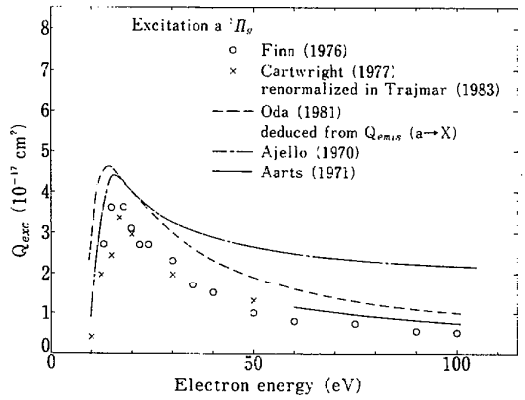

FIG. 7.4. Cross sections for the electronic excitation from the ground state to $a\ ^1\Pi_g$. Circles and crosses are from the energy loss measurements by, respectively, Finn and Doering (Ref. 51) and Cartwright *et al.* (Ref. 30) (renormalized by Trajmar *et al.*, Ref. 124). Solid and dot-dashed lines show, respectively, the values derived from the emission cross sections of Aarts and de Heer (Ref. 2) and Ajello (Ref. 4), both of which are presented in Fig. 7.3. Dashed line is the Born cross section derived by Oda and Osawa (Ref. 88).

(3) $a\ ^1\Pi_g$

The emission cross sections[2,4,60] for the 1384 Å line in the transition $a\ ^1\Pi_g$–$X^1\Sigma_g^+$ (Lyman–Birge–Hopfield system) are shown in Fig. 7.3. The high-energy part of Ajello's[4] cross section is in large disagreement with those of Aarts and de Heer and those of Holland. Aarts and de Heer[2] confirmed that their cross section behaves like the Bethe asymptote. The high-energy part of Ajello's data, therefore, may be in error. The excitation cross section derived from the Q_{emis} of Ajello and that of Aarts and de Heer are shown in Fig. 7.4 together with the two sets of ELS measurements.[30,51] Also shown are the Born cross section determined by Oda and Osawa[88] with the use of their measured values of generalized oscillator strengths. All the cross sections, except for the high-energy part of Ajello's, are in good agreement. This agreement supports the assumption that the cascade contribution to the emission of 1384 Å line is likely to be small.

(4) $C\ ^3\Pi_u$

The emission cross sections[64,103,104] measured for the 3371 and 3804 Å lines in the transition $C\ ^3\Pi_u$–$B\ ^3\Pi_g$ (second positive system) are shown in Fig. 7.5. Aarts and de Heer[1] also measured the emission cross section for 3371 Å line, which almost coincides with the data by Imami and

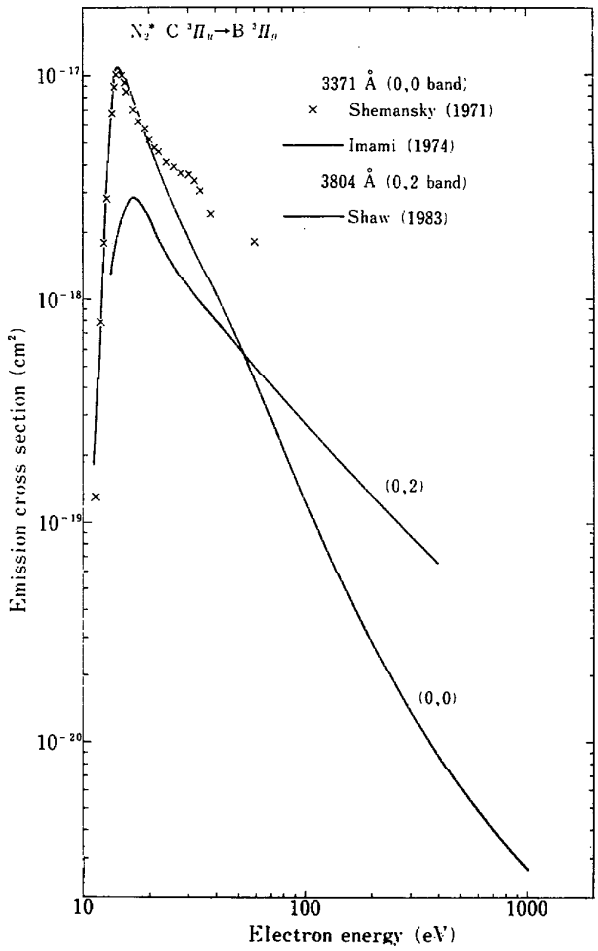

FIG. 7.5. Emission cross sections for the 3371 and 3804 Å lines in the second positive system ($C\ ^3\Pi_u$→$B\ ^3\Pi_g$) of N_2, measured by Shemansky and Broadfoot (Ref. 104), Imami and Borst (Ref. 64), and Shaw and Campos (Ref. 103).

Borst.[64] The enhancement of the cross section by Shemansky and Broadfoot[104] at the energies higher than 20 eV may be due to the effect of secondary electrons. The energy dependences of the Q_{emis} for 3371 Å (0–0 band) and 3804 Å (0–2 band) should coincide. The difference shown in Fig. 7.5 may be ascribed to experimental errors. The excitation cross sections derived from the Q_{emis} of Imami and Borst[64] and that of Shaw and Campos[103] are compared in Fig. 7.6 with the ELS measurement by Cartwright *et al.*[30] The Q_{exc} deduced from the Q_{emis} of Imami and Borst is in close agreement with the value of Cartwright *et al.*, but that from the data by Shaw and Campos deviates much from the two sets of Q_{exc}. From this it is more likely that the energy dependence of the Q_{emis} of Shaw and Campos is in error.

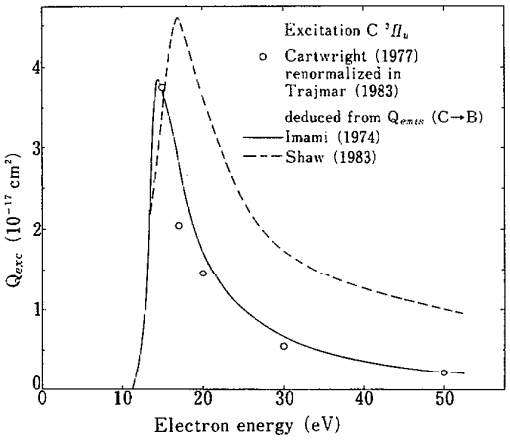

FIG. 7.6. Cross sections for the electronic excitation from the ground state to $C\,^3\Pi_u$. Circles are from the energy-loss measurement by Cartwright *et al.* (Ref. 30) (renormalized by Trajmar *et al.*, Ref. 124). Solid and dashed lines show, respectively, the values derived from the emission cross sections of Imami and Borst (Ref. 64) and Shaw and Campos (Ref. 103), both of which are given in Fig. 7.5.

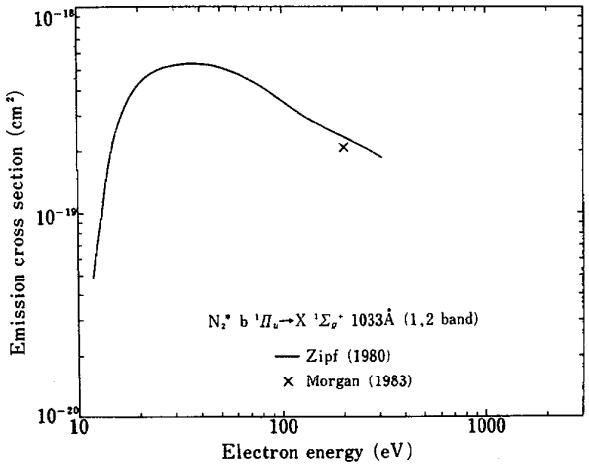

FIG. 7.8. Emission cross sections for the 1033 Å line in the Birge–Hopfield system ($b\,^1\Pi_u \rightarrow X\,^1\Sigma_g^+$) of N_2, measured by Zipf and Gorman (Ref. 137) and Morgan and Mentall (Ref. 82).

(5) $E\,^3\Sigma_g^+$

The excitation cross section measured by Cartwright *et al.*[30] is shown in Fig. 7.7. By the method of a surface detection of metastable molecules, Borst *et al.*[18] obtained cross sections having a narrow, very sharp peak just above the threshold. The cross section of Borst *et al.* has a maximum value of $(7.0 \pm 4.0) \times 10^{-18}$ cm^2 at the electron energy of 12.2 eV. Cartwright *et al.* did not measure the electron energy loss in that region of energy and provided no information about such a sharp structure. This structure can be attributed to a resonance (see the review by Schulz[101]). A further study is needed to obtain more definite quantitative information about the resonance cross section.

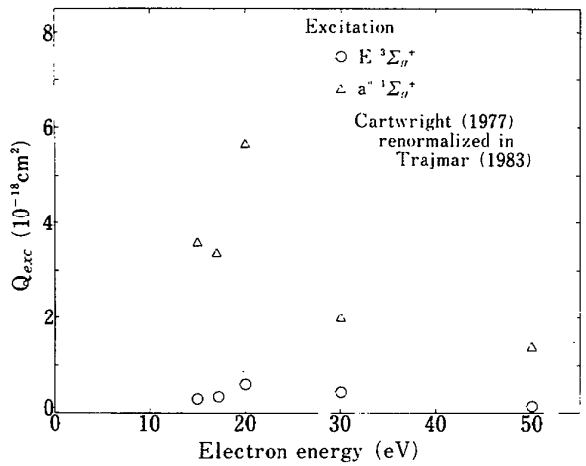

FIG. 7.7. Cross sections for the electronic excitations from the ground state to $E\,^3\Sigma_g^+$ and $a''\,^1\Sigma_g^+$, measured by Cartwright *et al.* (Ref. 30) and renormalized by Trajmar *et al.* (Ref. 124).

(6) $b\,^1\Pi_u$

The emission cross sections[82,137] for the 1033 Å line in the transition $b\,^1\Pi_u$–$X\,^1\Sigma_g^+$ (Birge–Hopfield system) are shown in Fig. 7.8. From these data the excitation cross section is derived as shown in Fig. 7.9. The energy dependence of the cross section obtained by the ELS method[33] is similar to the Q_{exc} thus derived. There is, however, a factor of 2 difference in the magnitudes of the two sets of cross sections. This discrepancy may be ascribed at least partly to the difficulty of the absolute measurement of Q_{emis}.

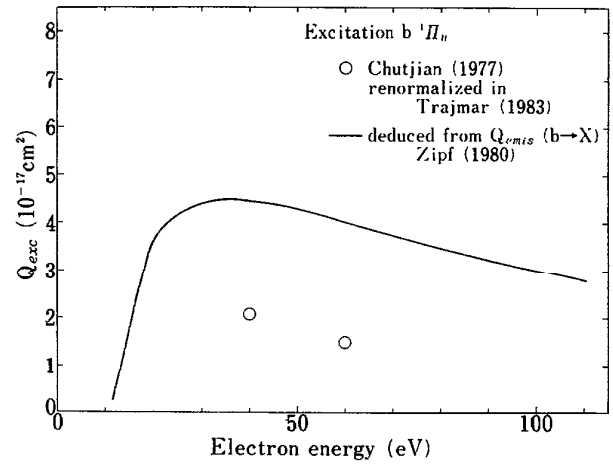

FIG. 7.9. Cross sections for the electronic excitation from the ground state to $b\,^1\Pi_u$. Circles are from the energy-loss measurement by Chutjian *et al.* (Ref. 33) (renormalized by Trajmar *et al.*, Ref. 124). Solid line shows the values derived from the emission cross section of Zipf and Gorman (Ref. 137), which is given in Fig. 7.8.

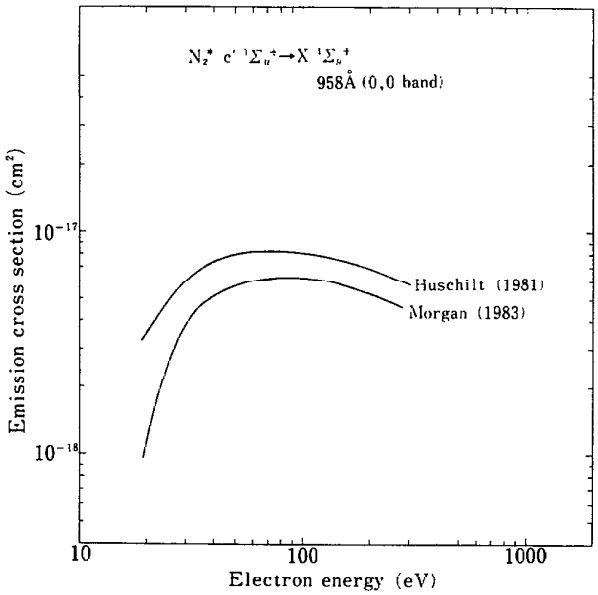

FIG. 7.10. Emission cross sections for the 958 Å line in the transition $c'\ ^1\Sigma_u^+ \rightarrow X\ ^1\Sigma_g^+$ of N_2, measured by Huschilt *et al.* (Ref. 63) and Morgan and Mentall (Ref. 82).

(7) $c'\ ^1\Sigma_u^+$

The emission cross sections[63,82] for the 958 Å line in the transition $c'\ ^1\Sigma_u^+ - X\ ^1\Sigma_g^+$ are shown in Fig. 7.10. The two sets of Q_{emis} in Fig. 7.10 are in fair agreement. The excitation cross section is derived from the Q_{emis} of Morgan and Mentall[82] and compared in Fig. 7.11 with that measured by Chutjian *et al.*[33] In this case the two sets of Q_{exc} have a similar magnitude but a very different energy dependence. The reason of the discrepancy is not known.

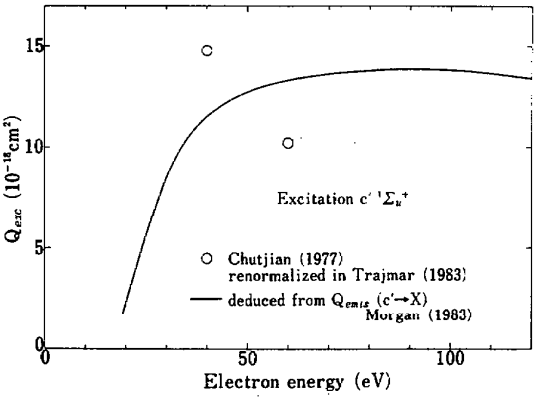

FIG. 7.11. Cross sections for the electronic excitation from the ground state to $c'\ ^1\Sigma_u^+$. Circles are from the energy-loss measurement by Chutjian *et al.* (Ref. 33) (renormalized by Trajmar *et al.*, Ref. 124). Solid line shows the values derived from the emission cross section of Morgan and Mentall (Ref. 82), which is shown in Fig. 7.10.

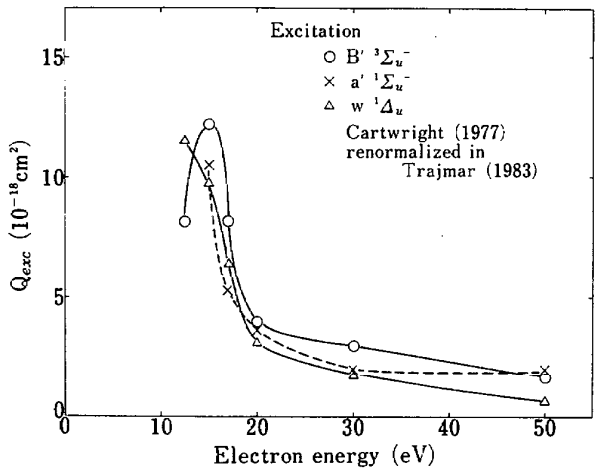

FIG. 7.12. Cross sections for the electronic excitations from the ground state to $B'\ ^3\Sigma_u^-$, $a'\ ^1\Sigma_u^-$, and $w\ ^1\Delta_u$, measured by Cartwright *et al.* (Ref. 30) and renormalized by Trajmar *et al.* (Ref. 124). Curves are drawn only for guiding eyes.

Table 7.2. Cross sections (in 10^{-18} cm^2) for the electronic excitation of N_2, measured by Chutjian et al. (1977) and renormalized by Trajmar et al. (1983)

State	Electron energy 40 eV	60 eV
F $^3\Pi_u$	1.42	1.03
G $^3\Pi_u$	2.96	1.71
b' $^1\Sigma_u^+$	13.4	7.25
c $^1\Pi_u$	9.57	7.87
o $^1\Pi_u$	2.25	1.96

(8) Other excited states

Cartwright *et al.*[30] and Chutjian *et al.*[33] reported the results of their measurements of excitation cross sections for a number of other states than mentioned above. Those are shown in Figs. 7.1, 7.7, 7.12, and Table 7.2.

8. Electron Collisions: Dissociative Processes (Excluding Dissociative Ionization)

8.1. Total Cross Section for Dissociation

Winters[133] obtained the total dissociation cross section by the measurement of the rate of adsorption of dissociative fragments on metal surfaces. His result is shown in Fig. 8.1. His cross section probably includes the contribution of dissociative ionization. The Winters cross section has some-

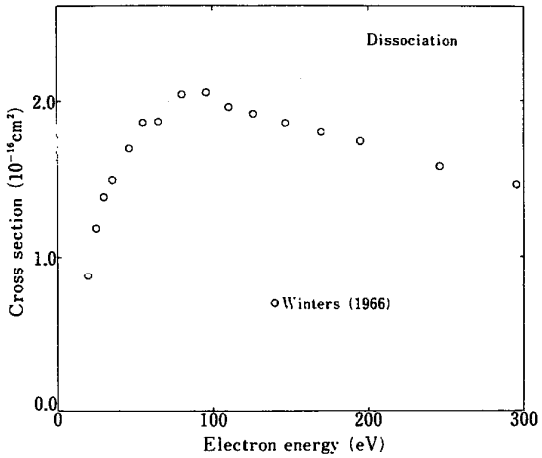

FIG. 8.1. Total dissociation cross section measured by Winters (Ref. 133).

times been criticized to be too large (e.g., Taniguchi *et al.*,[120] Hayashi *et al.*[58]). The cross section for dissociation (including dissociative ionization) should be smaller than the total excitation cross section (including dissociative ionization) defined by

$$Q_{T,exc} = Q_T - Q_{elas} - Q_{ion}(N_2^+) . \quad (8.1)$$

We can estimate $Q_{T,exc}$ with the use of the data on Q_T and Q_{elas} in Fig. 4.1 and $Q_{ion}(N_2^+)$ in Fig. 9.1. When compared with the $Q_{T,exc}$ thus determined, Winters' Q_{diss} is larger than the $Q_{T,exc}$ at the energies higher than 100 eV. The discrepancy amounts to about 70% at 300 eV. All the cross sections on the right-hand side of Eq. (8.1) have a good accuracy so that the $Q_{T,exc}$ has an uncertainty of at most about 20%. This suggests that Winters' cross section includes contributions from some other processes than the pure dissociation at least at the higher energies.

8.2. Production of Excited Nitrogen Atoms (Emission Cross Sections)

There are a number of papers reporting the measurement of the emission from the fragment atom. A list of the emission cross sections reported is given in Table 8.1. This table excludes those measurements which give a cross section at only one point of electron energy. Morgan and Mentall,[82] for instance, report emission cross sections for several lines at 200 eV of electron energy. We show in Figs. 8.2–8.5 the cross sections whose maximum value exceeds 10^{-18} cm^2. For the other cross sections, we only indicate their maximum values in Table 8.1.

Duplicate measurements were done for a few cases. In Fig. 8.3, for instance, three sets of cross sections are plotted for the emission of 1200 Å line. There is about a factor of 2 discrepancy among the different measurements. As noted in Sec. 7, it is very difficult to obtain accurate absolute magnitude for the emission cross sections. The discrepancy in Fig. 8.3 indicates the degree of reliability of the emission cross sections reported.

Table 8.1. List of the measured cross sections for the emission from nitrogen atoms upon electron-impact dissociation of N_2

Wavelength (Å)	Transition	AP[a] (eV)	E_{max}[b] (eV)	$Q(E_{max})$[c] (10^{-18}cm^2)	Reference[d]
1134	$2p^4\ ^4P\text{-}2p^3\ ^4S$	20.6	See Fig. 8.2		AD
1164	$3d\ ^2D\text{-}2p^3\ ^2D$	25.1	80	0.73	AD
1177	$4s\ ^2P\text{-}2p^3\ ^2D$	25.0	100	0.44	AD
1200	$3s\ ^4P\text{-}2p^3\ ^4S$	20.1	See Fig. 8.2,3		A,AD,MZ
1243	$3s'\ ^2D\text{-}2p^3\ ^2D$	24.4	See Fig. 8.2		AD,MZ
1494	$3s\ ^2P\text{-}2p^3\ ^2D$	20.5	See Fig. 8.2,4		A,AD,MZ
1743	$3s\ ^2P\text{-}2p^3\ ^2P$	20.5	See Fig. 8.5		A
4100	$3p'\ ^2D_{3/2}\text{-}3s\ ^2P_{1/2}$	22.7	78	0.018	F
4151	$4p\ ^4S_{3/2}\text{-}3s\ ^4P_{5/2}$	22.7	74	0.013	F
4935	$4p\ ^2S_{1/2}\text{-}3s\ ^2P_{3/2}$	23.5	78	0.033	F
5281	$4p\ ^4P_{5/2}\text{-}2p^4\ ^4P_{5/2}$	22.7	86	0.009	F
5329	$4p\ ^4D_{7/2}\text{-}2p^4\ ^4P_{5/2}$	22.7	81	0.016	F
6485	$4d\ ^4F_{7/2}\text{-}3p\ ^4D_{5/2}$	24.0	97	0.034	F
7424	$3p\ ^4S_{3/2}\text{-}3s\ ^4P_{1/2}$	22.6	88	0.130	F
8216	$3p\ ^4P_{5/2}\text{-}3s\ ^4P_{5/2}$	22.5	82	0.820	F
8629	$3p\ ^2P_{3/2}\text{-}3s\ ^2P_{3/2}$	22.3	85	0.470	F
8680	$3p\ ^4D\text{-}3s\ ^4P$	21.5	See Fig. 8.2,5		AD,F
9047	$3p'\ ^2F\text{-}3s'\ ^2D$	23.4	84	0.200	F
9060	$3d\ ^2D_{3/2}\text{-}3p\ ^2S_{1/2}$	23.2	84	0.071	F
9393	$3p\ ^2D_{5/2}\text{-}3s\ ^2P_{3/2}$	21.7	85	0.703	F
10114	$3d\ ^4F\text{-}3p\ ^4D$	23.0	81	0.550	F
10540	$3d\ ^4D\text{-}3p\ ^4P$	22.7	83	0.301	F

[a]Appearance potential.

[b]Electron energy at which the cross section has its maximum.

[c]Maximum of the emission cross section.

[d]A: Ajello (1970); AD: Aarts and de Heer (1971); F: Filippelli et al. (1982); MZ: Mumma and Zipf (1971).

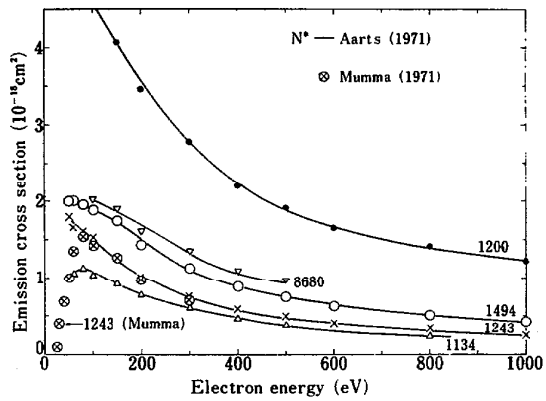

FIG. 8.2. Cross sections for the line emissions from nitrogen atoms upon electron-impact dissociation of N_2. Numbers along the data points indicate the wavelength (in Å) of the line measured (see Table 8.1).

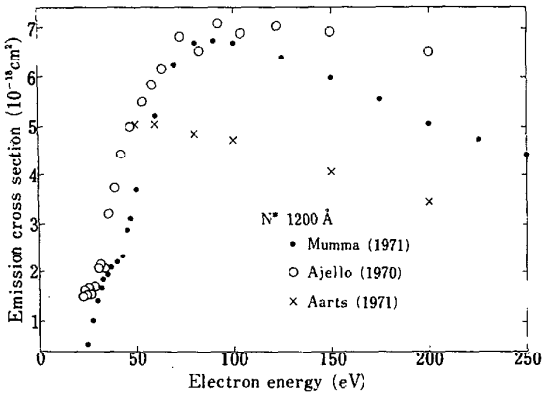

FIG. 8.3. Same as Fig. 8.2, but for the emission of 1200 Å line.

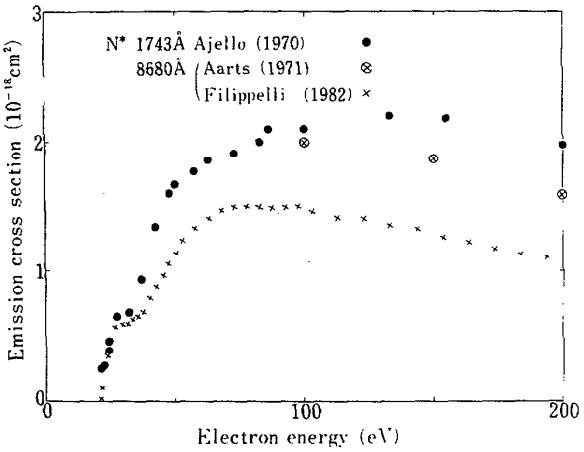

FIG. 8.5. Same as Fig. 8.2, but for the emissions of 1743 and 8680 Å lines.

Recently interest has been increased in the highly excited atoms produced by electron-impact dissociation of molecules. There are several papers on the production of highly excited nitrogen atoms from N_2.[89,100,129] Schiavone *et al.*[100] found that the cross section for the formation of the highly excited atom with its principal quantum number n can be approximated by

$$Q_{\text{diss}}[\text{N}(n)] = 1.6\times10^{-16}\ \text{cm}^2/n^3, \qquad (8.2)$$

for $n = 15$–80 at the electron energy of 100 eV. The energy dependence of the cross section is also discussed by them.

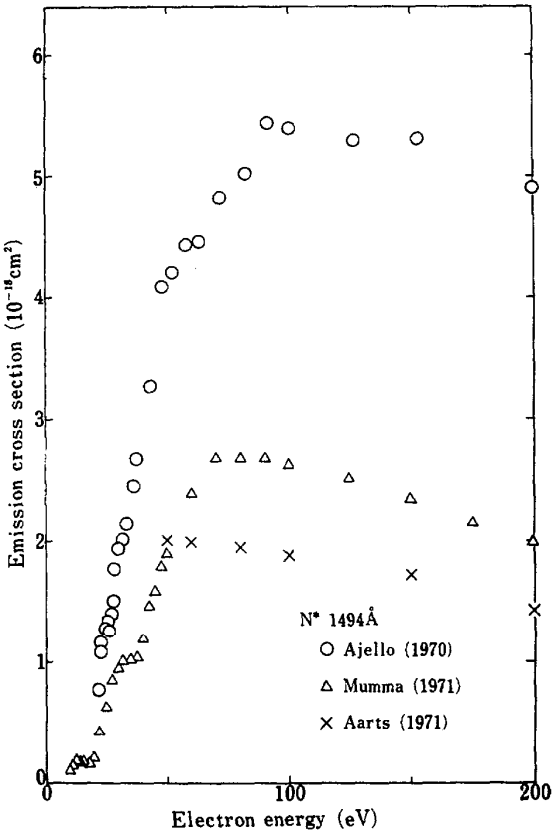

FIG. 8.4. Same as Fig. 8.2, but for the emission of 1494 Å line.

9. Electron Collisions: Ionization (Including Dissociative Ionization)

9.1. Cross Sections for Ion Production

a. Gross Ionization Cross Section

A measurement of ion current gives the gross (or total) ionization cross section defined by

$$Q_{\text{ion}}(\text{gross}) = \sum_n nQ_{\text{ion}}(\text{N}_2^{n+}) + \sum_m mQ_{\text{ion}}(\text{N}^{m+}). \qquad (9.1)$$

Here, $Q_{\text{ion}}(\text{N}_2^{n+})$ is the cross section for the production of n-fold ionized ions of N_2, and $Q_{\text{ion}}(\text{N}^{m+})$ is that for the disso-

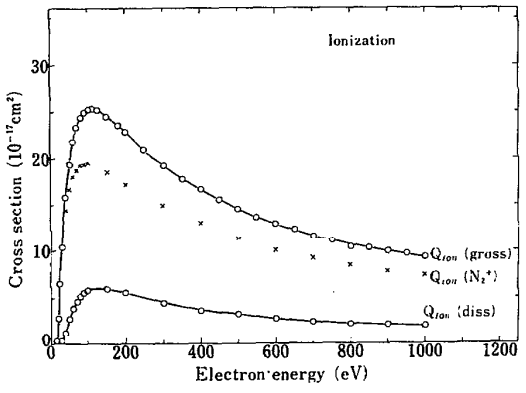

FIG. 9.1. Electron-impact ionization cross sections of N_2. Q_{ion} (gross): gross ionization cross section; $Q_{\text{ion}}(N_2^+)$: cross section for the production of N_2^+; Q_{ion} (diss): dissociative ionization cross section.

ciative ionization producing N^{m+}. Among many measurements, the result by Rapp and Englander-Golden[96] has been often taken as the standard for Q_{ion} (gross) of N_2. A recent review by de Heer and Inokuti,[42] for instance, concluded that the data by Rapp and Englander-Golden[96] are most likely to be right within the stated limit of errors (7%), and no recent work has substantially reduced the error limit. Figure 9.1 shows the Q_{ion} (gross) of Rapp and Englander-Golden.[96]

b. Production of N_2^+ and N_2^{++}

Märk[75] reported the cross section for the production of N_2^+ and N_2^{++}. He detected each ion with a mass spectrometer. He compared his result of $Q_{ion}(N_2^+) + 2Q_{ion}(N_2^{++})$ with that derived from the measurement by Rapp and Englander-Golden.[96] The latter values are obtained by a subtraction of the dissociative ionization cross section measured by Rapp *et al.*[97] from the Q_{ion} (gross) in Fig. 9.1. It turned out that the Märk result deviated significantly from that of Rapp. The maximum difference occurs around about 50 eV, where the Märk value is only about 65% of the Rapp one. Märk obtained his absolute magnitude by normalizing his relative measurement to the ionization cross section of Ar, which was also shown in his paper. The ionization cross section of Ar used by Märk, however, is systematically different from that reported later by the same group.[113] At about 50 eV, for instance, the new measurement of the Ar ionization cross section exceeds the old data by about 34%. The values of Q_{ion} reported by Märk,[75] therefore, may be of some systematic error at least in the region of lower electron energies. If the correction factor for the Ar data can be applied to N_2, the difference between the two measurements[75,96] is reduced to about 13%. This was pointed out first by Armentrout *et al.*[8]

Here we calculate $Q_{ion}(N_2^+)$ from the relation

$$Q_{ion}(N_2^+) = Q_{ion}(\text{gross}) - Q_{ion}(\text{diss}), \qquad (9.2)$$

with Q_{ion} (gross) and Q_{ion} (diss) shown in Fig. 9.1 (the latter cross section being discussed in the next subsection). The result is also shown in Fig. 9.1.

In the relation (9.2), we ignored the contribution of N_2^{++} to the gross ionization. As the ratio $Q_{ion}(N_2^{++})/Q_{ion}(N_2^+)$ is a few percent (see, e.g., Märk[75]), the contribution of N_2^{++} can be neglected within the error limit (7%) of Q_{ion} (gross). A very similar procedure was taken by Armentrout *et al.*[8] to derive their result of $Q_{ion}(N_2^+)$, although it is only given up to 240 eV. They took account of the contribution of N_2^{++} using Märk's data. Their values agree with ours within a few percent.

c. Dissociative Ionization

Rapp *et al.*[97] measured the dissociative ionization cross section defined by

$$Q_{ion}(\text{diss}) = Q_{ion}(N^+) + 2Q_{ion}(N^{++}). \qquad (9.3)$$

Their values have to be corrected relative to two parameters: they detected only the fragment ions having kinetic energy larger than 0.25 eV and they used the McLeod gauge to measure the pressure of the target gas. Following Armentrout *et al.*,[8] we increased the Q_{ion} (diss) measured by Rapp *et al.*[97] by 5% to correct for the fragment ions with lower velocities and decreased that by 8.8% to correct the pressure gauge. The resulting values of Q_{ion} (diss) are presented in Figs. 9.1 and 9.2.

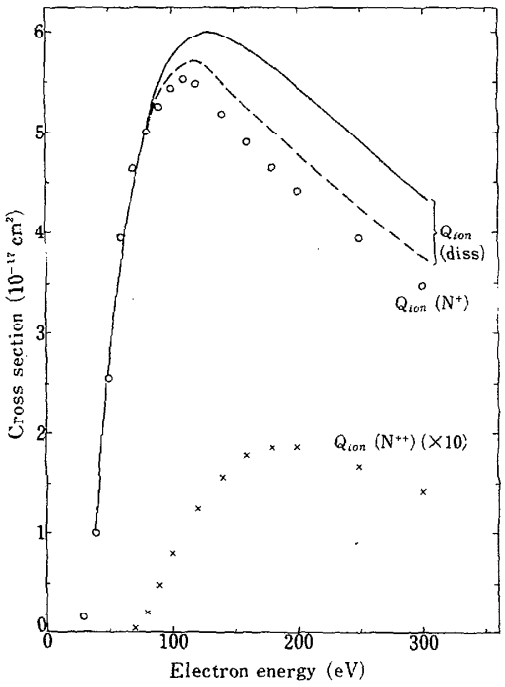

FIG. 9.2. Cross sections for the dissociative ionization [$Q_{ion}(N^+)$ for the production of N^+ and $Q_{ion}(N^{++})$ for the production of N^{++}], measured by Crowe and McConkey (Ref. 39). For $Q_{ion}(N^{++})$, 10 times the measured values are plotted for illustration. Also plotted are Q_{ion} (diss) derived from the data by Crowe and McConkey (dashed line) and those by Rapp *et al.* (Ref. 97) (solid line).

Crowe and McConkey[39] measured N^+ and N^{++} separately. Figure 9.2 shows their cross sections $Q_{ion}(N^+)$ and $Q_{ion}(N^{++})$. They obtained the cross sections by normalizing, at 100 eV, their data on Q_{ion} (diss) [$= Q_{ion}(N^+) + 2Q_{ion}(N^{++})$] to that of Rapp *et al.*[97] In so doing they reduced the Q_{ion} (diss) of Rapp *et al.* by 7.7% to take account of the pressure-gauge correction. They ignored the correction for slow ions. The Q_{ion} (diss) obtained by Crowe and McConkey[39] is also plotted in Fig. 9.2 and compared with the Q_{ion} (diss) derived above from the data by Rapp *et al.*[97] The difference (up to 15% at 300 eV) between the two sets of Q_{ion} (diss) probably indicates the uncertainty of the present Q_{ion} (diss).

9.2. Production of Excited Ions from N_2

a. Production of Excited States of N_2^+

A number of papers reported the measurement of emission from N_2^+ at the impact of electrons with N_2. Figure 9.3

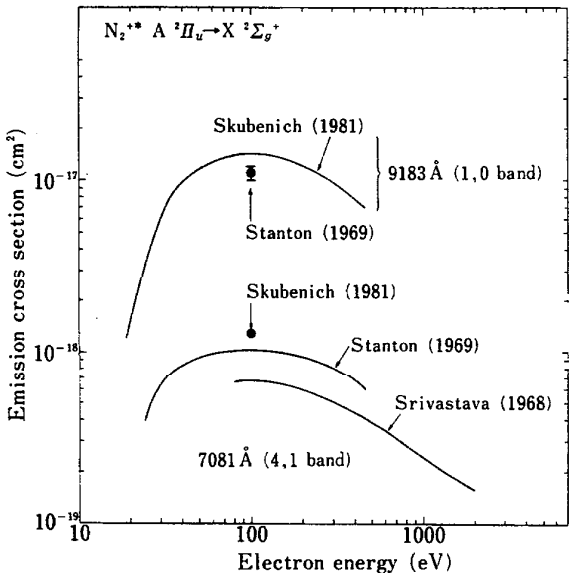

FIG. 9.3. Emission cross sections for the 9183 and 7081 Å lines in the Meinel system (A $^2\Pi_u \rightarrow$X $^2\Sigma_g^+$) of N_2^+, measured at the collision of electrons with N_2 by Skubenich and Zapesochnyy (Ref. 109), Stanton and St. John (Ref. 112), and Srivastava and Mirza (Ref. 110).

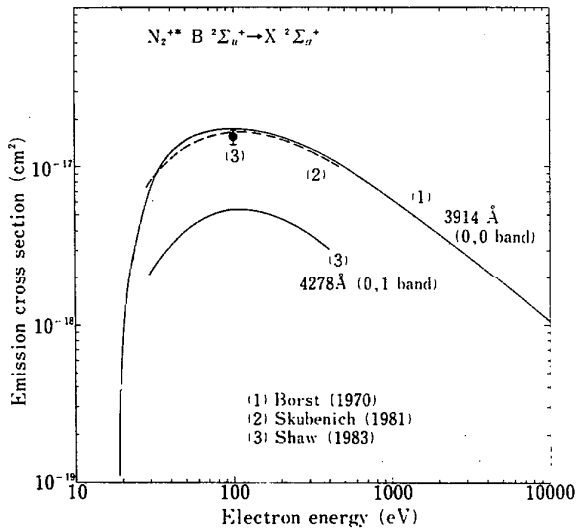

FIG. 9.5. Emission cross sections for the 3914 and 4278 Å lines in the first negative system (B $^2\Sigma_u^+ \rightarrow$X $^2\Sigma_g^+$) of N_2^+, measured at the collision of electrons with N_2 by (1) Borst and Zipf (Ref. 17), (2) Skubenich and Zapesochnyy (Ref. 109), and (3) Shaw and Campos (Ref. 103).

gives the emission cross sections[109,110,112] for the 7081 and 9183 Å lines in the transition A $^2\Pi_u - $X $^2\Sigma_g^+$ of N_2^+ (Meinel system). From the Q_{emis} of Skubenich and Zapesochnyy[109] the cross section for the production of A $^2\Pi_u$ state of N_2^+ has been deduced with the use of the procedure similar to that in the case of excitation of N_2 (see Sec. 7). The result is shown in Fig. 9.4. Shemansky and Broadfoot[104] reported the excitation cross section derived in a similar way. Their result is compared in Fig. 9.4 to the present one.

There have been a large number of measurements of the emission from B $^2\Sigma_u^+$ state of N_2^+. Some representative data on the emission cross section for the B $^2\Sigma_u^+ -$X $^2\Sigma_g^+$ transition (1st negative system) are presented in Fig. 9.5. The data by Borst and Zipf[17] have been taken as the standard among various emission cross sections.[78] From their data, we have derived the excitation cross section for N_2^+ (B $^2\Sigma_u^+$) as shown in Fig. 9.6. The resulting value of Q_{exc} is almost 10%

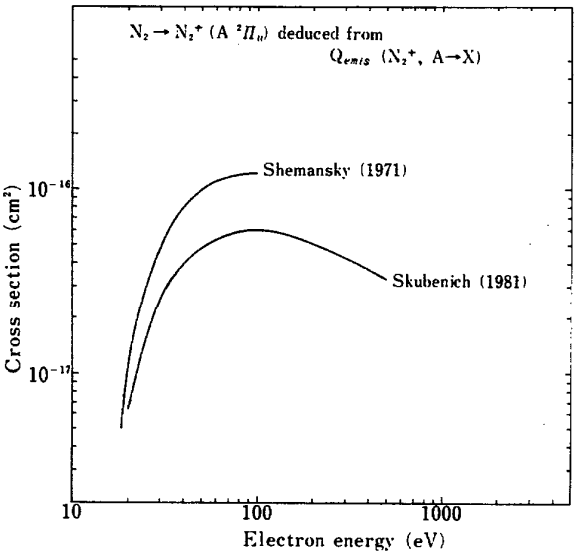

FIG. 9.4. Cross sections for the production of N_2^+ in its A $^2\Pi_u$ state at the collision of electrons with N_2. The values derived from the emission cross sections (Refs. 104 and 109) are shown.

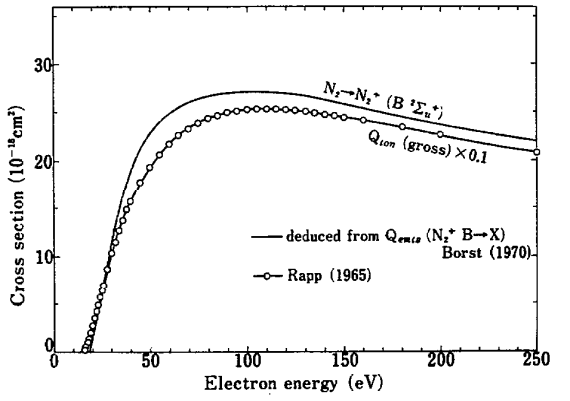

FIG. 9.6. Cross section for the production of N_2^+ in its B $^2\Sigma_u^+$ state at the collision of electrons with N_2. The values have been deduced from the emission cross section of Borst and Zipf (Ref. 17), which is given in Fig. 9.5. For comparison, one-tenth the value of the gross ionization cross section shown in Fig. 9.1 is plotted.

Table 9.1. List of the measured cross sections for the emission from N^+ upon electron-impact dissociative ionization of N_2

Wavelength (Å)	Transition	AP[a] (eV)	E_{max}[b] (eV)	$Q(E_{max})$[c] (10^{-18} cm^2)	Ref[d]
747	$3s\ ^1P\text{-}2p^2\ ^1D$	45.0	150	0.153	AD
776	$2p^3\ ^1D\text{-}2p^2\ ^1D$	44.4	150	0.116	AD
916	$2p^3\ ^3P\text{-}2p^2\ ^3P$	37.7	140	0.508	AD,MM
1084	$2p^3\ ^3D\text{-}2p^2\ ^3P$	35.6	See Fig. 9.7		AD
5001	$3d\ ^3F\text{-}3p\ ^3D$	56.5	168	0.150	F
5680	$3p\ ^3D_3\text{-}3s\ ^3P_2$	53.8	170	0.230	F

[a] Appearance potential.

[b] Electron energy at which the cross section has its maximum.

[c] Maximum of the emission cross section.

[d] AD: Aarts and de Heer (1971); F: Filippelli et al. (1982); MM: Morgan and Mentall (1983)

of the Q_{ion} (gross) for a wide range of electron energies above 50 eV.

Ajello[4] has tried to measure the emission from N_2^+ ($C\ ^2\Sigma_u^+$), but got no signal. He concluded that the upper limit of Q_{emis} for $C\ ^2\Sigma_u^+$ state is 3×10^{-20} cm^2.

b. Production of N^+ in its Excited State

Emissions from the fragment ion (N^+) were measured by several people. Table 9.1 lists the lines measured. As in the case of N, Table 9.1 excludes those measurements which give the cross section at only one point of energy. Morgan and Mentall,[82] for instance, give the cross section for several lines at 200 eV. In Fig. 9.7, the emission cross section for the 1084 Å line is shown. Other lines have a cross section less than 10^{-18} cm^2. The accuracy of these cross sections would be the same as in the case of N (see Sec. 8.2).

9.3. Energy Distribution of Secondary Electrons

Energy distribution of secondary (ejected and scattered) electrons is needed when we determine the energy loss of electrons upon ionizing collisions with nitrogen molecules. Opal *et al.*[95] reported the result of their measurement for the incident energies from 50 to 2000 eV. Their results are shown in Figs. 9.8a and 9.8b. After the publication of the paper, some other measurements were done. DuBois and Rudd[48] and Shyn[107] reported their results for 100–500 eV and for 50–400 eV, respectively. The data of Opal *et al.*[95] are in good agreement with the recent ones at 100, 200, and 500 eV. At 50 eV, the data by Opal *et al.* are by about 50% less than those of Shyn.[107] As it is difficult to measure low-energy electrons, this discrepancy may be ascribed to experimental uncertainties. Opal *et al.* claimed their maximum error to be about 30%.

The measurement by Opal *et al.* was restricted to the secondary electrons with energies above 4 eV. On consideration of Shyn's data, which extended the energy down to 1 eV, a smooth extrapolation is likely to be made to the lower energy. Actually Opal *et al.*[95] proposed to use a simple form,

$$\frac{dQ_{ion}}{dE_s} = \frac{C}{E_s^2 + \hat{E}^2} \quad \text{with } \hat{E} = 11.4 \text{ eV}, \tag{9.4}$$

for the differential cross section over the secondary electron energy E_s (in eV). Here C is a constant depending on the energy of the incident electron. Recently Goruganthu *et al.*[53] reported their measurement of low-energy secondary electrons at the incidence of 1000 eV electrons. They showed a significant peaking of the differential cross section at the lowest energy ($\sim$1 eV) measured. They ascribed it to the effect of autoionization. Thus one should be careful when an extrapolation is made of the differential cross section obtained by Opal *et al.*[95]

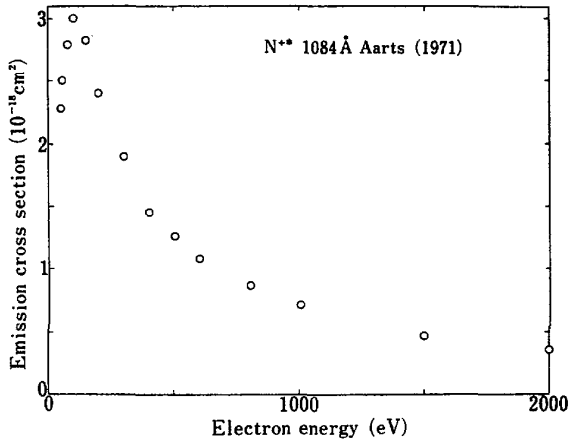

FIG. 9.7. Emission cross section for the 1084 Å line from N^+ measured at the electron collision with N_2 (Ref. 2).

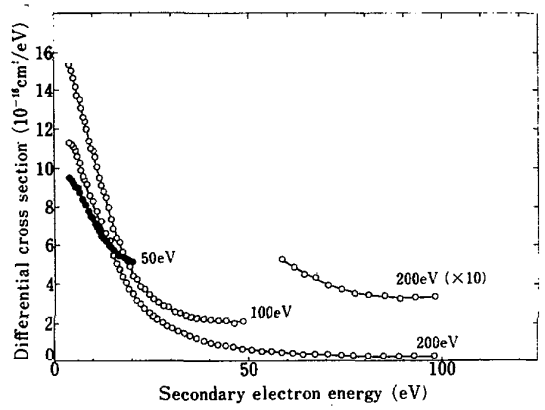

FIG. 9.8a. Energy distribution of the secondary electrons at the ionizing collisions of electrons with N_2. Energy of the incident electron is indicated along each curve (Ref. 95).

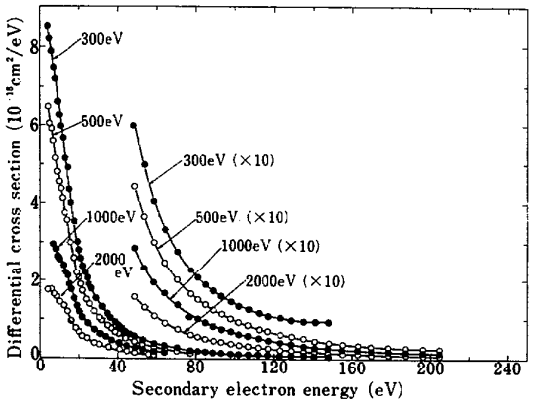

FIG. 9.8b. Energy distribution of the secondary electrons at the ionizing collisions of electrons with N_2. Energy of the incident electron is indicated along each curve (Ref. 95).

10. Summary and Future Problems

Cross sections for electron collisions with nitrogen molecules are summarized in Fig. 10.1. Data sources are: the total (Q_T), elastic (Q_{elas}) and momentum-transfer (Q_m) cross sections from Fig. 4.1, the cross section for the rotational excitation $J = 0 \rightarrow 2$ [$Q_{rot}(0 \rightarrow 2)$] from Fig. 5.1, the cross section for the vibrational excitation $v = 0 \rightarrow 1$ [$Q_{vib}(0 \rightarrow 1)$] from Figs. 6.1 and 6.2, a few representative cross sections for electronic excitations from Figs. 7.1 and 7.4, the gross and dissociative ionization cross sections from Fig. 9.1. The reliability of each cross section has been discussed in the respective sections.

The cross section data on the collisions of photons and electrons with nitrogen molecules have increased both in quantity and in quality these 10 years. An extensive measurement of electron energy-loss spectra, for instance, has been done to provide vibrational and electronic excitation

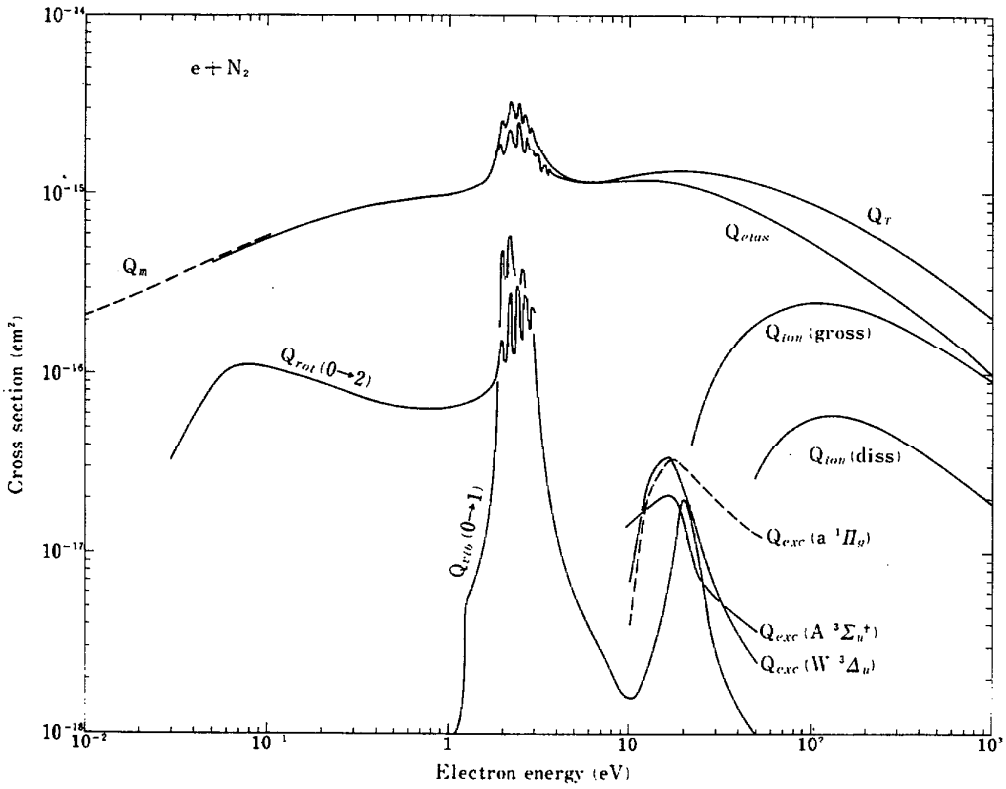

FIG. 10.1. Summary of the cross sections for the electron collision with N_2.

cross sections. The total scattering cross sections have been obtained with an error of a few percent. Experimental information, though fragmentary, is now available for rotational transitions. As shown in the previous sections, however, we are still far from the stage where a comprehensive set of accurate cross sections is at hand for any application. Considerable work remains to be done. In particular we need more research on the following collision processes:

(a) Electron-impact excitation of electronic states.

The JPL group published their measurement of the cross sections for 17 excited states. The measurements, however, were limited to the collision energies less than 60 eV. Furthermore the cross sections for seven states were obtained only at two energies. Data on the excitation cross sections are urgently needed over a wider range and finer grid of energy. The ELS measurement of the JPL group was done for loss energy less than 14.2 eV. Cross sections for excitation processes with thresholds higher than 14.2 eV should be investigated.

(b) Dissociation to ground-state and metastable-state atoms by electron and photon collisions.

There is no definite information about the magnitude of the dissociation cross section for the production of nitrogen atoms in their ground state. Since ground-state nitrogen atoms are difficult to detect, a new technique must be devised. Also important are the cross sections for the production of nitrogen atoms in their metastable states, i.e., $N(^2P$ or $^2D)$.

(c) Electron-impact excitation of vibrational states at low energies.

Vibrational excitation is the most efficient energy-loss process in the region from the threshold to about 10 eV. Though much study has been done, reliable information about the absolute magnitude of the cross section is fragmentary. In particular, more beam data must be obtained below the 2.3 eV shape resonance.

(d) Electron-impact excitation of rotational states.

As is shown in Sec. 5, we now have a comprehensive result of calculation of rotational transitions at 0.03–3 eV. This result should be tested by experiment. Furthermore the preliminary experimental data at higher energies (5–20 eV) have to be confirmed.

After some or all of the above tasks are completed, the present data compilation will be revised.

11. Acknowledgments

During the course of this data compilation, many collegues provided us with valuable information about the data presented here. Particular thanks are due to A. Crowe, P. M. Dehmer, H. Ehrhardt, P. Gürtler, K. Jost, C. C. Lin, J. A. R. Samson, H. Tanaka, S. Trajmar, and H. F. Winters, who made available to us unpublished results or detailed numerical values of the published data.

12. References

[1] J. F. M. Aarts and F. J. de Heer, Chem. Phys. Lett. **4**, 116 (1969).
[2] J. F. M. Aarts and F. J. de Heer, Physica **52**, 45 (1971).
[3] J. H. Agee, J. B. Wilcox, L. E. Abbey, and T. F. Moran, Chem. Phys. **61**, 171 (1981).
[4] J. M. Ajello, J. Chem. Phys. **53**, 1156 (1970).
[5] M. Allan, J. Phys. B **18**, 4511 (1985).
[6] G. R. Alms, A. K. Burnham, and W. H. Flygare, J. Chem. Phys. **63**, 3321 (1975).
[7] R. Anderson, At. Data **3**, 227 (1971).
[8] P. B. Armentrout, S. M. Tarr, A. Sori, and R. S. Freund, J. Chem. Phys. **75**, 2786 (1981).
[9] C. Asawaroengchai and G. M. Rosenblatt, J. Chem. Phys. **72**, 2664 (1980).
[10] W. Benesch, Phys. Rev. A **19**, 445 (1979).
[11] J. Berkowitz, *Photoabsorption, Photoionization, and Photoelectron Spectroscopy* (Academic, New York, 1979).
[12] M. Berman, H. Estrada, L. S. Cederbaum, and W. Domcke, Phys. Rev. A **28**, 1363 (1983).
[13] A. Bianconi, H. Petersen, F. C. Brown, and R. Z. Bachrach, Phys. Rev. A **17**, 1907 (1978).
[14] G. Birnbaum and E. R. Cohen, Mol. Phys. **32**, 161 (1976).
[15] H. J. Blaauw, F. J. de Heer, R. W. Wagenaar, and D. H. Barends, J. Phys. B **10**, L299 (1977).
[16] W. L. Borst, Phys. Rev. A **5**, 648 (1972).
[17] W. L. Borst and E. C. Zipf, Phys. Rev. A **1**, 834 (1970).
[18] W. L. Borst, W. C. Wells, and E. C. Zipf, Phys. Rev. A **5**, 1744 (1972).
[19] N. J. Bridge and A. D. Buckingham, Proc. R. Soc. London Ser. A **295**, 334 (1966).
[20] J. P. Bromberg, J. Chem. Phys. **52**, 1243 (1970).
[21] A. D. Buckingham, R. L. Disch, and D. A. Dunmur, J. Am. Chem. Soc. **90**, 3104 (1968).
[22] B. D. Buckley and P. G. Burke, J. Phys. B **10**, 725 (1977).
[23] F. E. Budenholzer, E. A. Gislason, A. D. Jorgensen, and J. G. Sachs, Chem. Phys. Lett. **47**, 429 (1977).
[24] M. A. Buldakov, I. I. Matrosov, and T. N. Popova, Opt. Spectrosc. **47**, 48 (1979).
[25] P. G. Burke, C. J. Noble, and S. Salvini, J. Phys. B **16**, L113 (1983).
[26] T. A. Carlson, M. O. Krause, D. Mchaffy, J. W. Taylor, F. A. Grimm, and J. D. Allen, Jr., J. Chem. Phys. **73**, 6056 (1980).
[27] V. L. Carter and J. Berkowitz, J. Chem. Phys. **59**, 4573 (1973).
[28] D. C. Cartwright and T. H. Dunning, Jr., J. Phys. B **7**, 1776 (1974).
[29] D. C. Cartwright, A. Chutjian, S. Trajmar, and W. Williams, Phys. Rev. A **16**, 1013 (1977).
[30] D. C. Cartwright, S. Trajmar, A. Chutjian, and W. Williams, Phys. Rev. A **16**, 1041 (1977).
[31] N. Chandra and A. Temkin, Phys. Rev. A **14**, 507 (1976).
[32] *Electron-Molecule Interactions and Their Applications*, edited by L. G. Christophorou (Academic, New York, 1984), Vols. 1 and 2.
[33] A. Chutjian, D. C. Cartwright, and S. Trajmar, Phys. Rev. A **16**, 1052 (1977).
[34] B. E. Cole and R. N. Dexter, J. Phys. B **11**, 1011 (1978).
[35] L. A. Collins, D. C. Cartwright, and W. R. Wadt, J. Phys. B **13**, L613 (1980).
[36] G. R. Cook, M. Ogawa, and R. W. Carlson, J. Geophys. Res. **78**, 1663 (1973).
[37] P. C. Cosby, R. Möller, and H. Helm, in *XIII ICPEAC Abstracts of Contributed Papers*, 1983, p. 56.
[38] R. W. Crompton, in *XVI ICPIG Invited Papers*, edited by W. Bötticher, H. Wenk, and E. Schulz-Gulde, Organizing Committee of ICPIG-XVI, 1983, p. 58.
[39] A. Crowe and J. W. McConkey, J. Phys. B **6**, 2108 (1973).
[40] G. Dalba, P. Fornasini, R. Grisenti, G. Ranieri, and A. Zecca, J. Phys. B **13**, 4695 (1980).
[41] A. Dalgarno and R. J. Moffett, Proc. Natl. Acad. Sci. India A **33**, 511 (1963).
[42] F. J. de Heer and M. Inokuti, in *Electron Impact Ionization*, edited by T. D. Märk and G. H. Dunn (Springer, Berlin, 1985), p. 232.
[43] P. M. Dehmer, P. J. Miller, and W. A. Chupka, J. Chem. Phys. **80**, 1030 (1984).
[44] D. R. Denne, J. Phys. D **3**, 1392 (1970).
[45] L. de Reilhac and N. Damany, J. Quant. Spectrosc. Radiat. Transf. **18**, 121 (1977).
[46] L. Dubé and A. Herzenberg, Phys. Rev. A **20**, 194 (1979).
[47] R. D. DuBois and M. E. Rudd, J. Phys. B **9**, 2657 (1976).
[48] R. D. DuBois and M. E. Rudd, Phys. Rev. A **17**, 843 (1978).
[49] A. G. Engelhardt, A. V. Phelps, and C. G. Risk, Phys. Rev. **135**, A1566 (1964).

[50]A. R. Filippelli, F. A. Sharpton, C. C. Lin, and R. E. Murphy, J. Chem. Phys. **76**, 3597 (1982).
[51]T. G. Finn and J. P. Doering, J. Chem. Phys. **64**, 4490 (1976).
[52]J. L. Gardner and J. A. R. Samson, J. Electron Spectrosc. **13**, 7 (1978).
[53]R. R. Goruganthu, W. G. Wilson, and R. A. Bonham, in Argonne National Laboratory Report No. ANL-84-28, 1984, p. 110.
[54]P. Gürtler, V. Saile, and E. E. Koch, Chem. Phys. Lett. **48**, 245 (1977).
[55]G. N. Haddad, Aust. J. Phys. **37**, 487 (1984).
[56]A. Hamnett, W. Stoll, and C. E. Brion, J. Electron Spectrosc. **8**, 367 (1976).
[57]M. Hayashi, Nagoya Univ. Report No. IPPJ-AM-19, 1981.
[58]M. Hayashi, J. Hamada, T. Asano, and M. Sakai, in Proceedings of the International Seminar on Swarm Experiments in Atomic Collision Research, 1979, p. 99.
[59]K. R. Hoffman, M. S. Dababneh, Y.-F. Hsieh, W. E. Kauppila, V. Pol, J. H. Smart, and T. S. Stein, Phys. Rev. A **25**, 1393 (1982).
[60]R. F. Holland, J. Chem. Phys. **51**, 3940 (1969).
[61]R. M. Holmes and G. V. Marr, J. Phys. B **13**, 945 (1980).
[62]K. P. Huber and G. Herzberg, *Molecular Spectra and Molecular Structure, IV. Constants of Diatomic Molecules* (Van Nostrand Reinhold, New York, 1979).
[63]J. C. Huschilt, H. W. Dassen, and J. W. McConkey, Can. J. Phys. **59**, 1893 (1981).
[64]M. Imami and W. L. Borst, J. Chem. Phys. **61**, 1115 (1974).
[65]M. Inokuti, Rev. Mod. Phys. **43**, 297 (1971).
[66]K. Jost, P. G. F. Bisling, F. Eschen, M. Felsmann, and L. Walther, in *XIII ICPEAC Abstracts of Contributed Papers*, 1983, p. 91, and private communications.
[67]K. Jung, T. Antoni, R. Müller, K.-H. Kochem, and H. Ehrhardt, J. Phys. B **15**, 3535 (1982).
[68]A. K. Kazanskii and I. I. Fabrikant, Sov. Phys. Usp. **27**, 607 (1984).
[69]R. E. Kennerly, Phys. Rev. A **21**, 1876 (1980).
[70]K. Kirby, E. R. Constantinides, S. Babeu, M. Oppenheimer, and G. A. Victor, At. Data Nucl. Data Tables **23**, 63 (1979).
[71]W. M. Kosman and S. Wallace, J. Chem. Phys. **82**, 1385 (1985).
[72]N. E. Kuz'menko, L. A. Kuznetsova, A. P. Monyakin, Yu. Ya. Kuzyakov, and Yu. A. Plastinin, Sov. Phys. Usp. **22**, 160 (1979).
[73]N. F. Lane, Rev. Mod. Phys. **52**, 29 (1980).
[74]A. Lofthus and P. H. Krupenie, J. Phys. Chem. Ref. Data **6**, 113 (1977).
[75]T. D. Märk, J. Chem. Phys. **63**, 3731 (1975).
[76]T. D. Märk and G. H. Dunn *Electron Impact Ionization*, edited by (Springer, Berlin, 1985).
[77]G. V. Marr, J. M. Morton, R. M. Holmes, and D. G. McCoy, J. Phys. B **12**, 43 (1979).
[78]J. W. McConkey, in Argonne National Laboratory Report No. ANL-84-28, 1984, p. 129.
[79]J. W. McConkey and F. R. Simpson, J. Phys. B **2**, 923 (1969).
[80]*Electron-Molecule Collisions and Photoionization Processes*, edited by V. McCoy, H. Suzuki, K. Takayanagi, and S. Trajmar (Verlag Chemie International, Deerfield Beach, 1983).
[81]H. H. Michels, in *The Excited State in Chemical Physics, Part 2*, edited by J. W. McGowan (Wiley, New York, 1981), p. 225.
[82]H. D. Morgan and J. E. Mentall, J. Chem. Phys. **78**, 1747 (1983).
[83]Y. Morioka, S. Aoyama, Y. Kageyama, T. Hayaishi, I. H. Suzuki, G. Isoyama, S. Asaoka, E. Ishiguro, and M. Nakamura, J. Phys. B **18**, 2795 (1984).
[84]M. A. Morrison and P. J. Hay, J. Chem. Phys. **70**, 4034 (1979).
[85]M. J. Mumma and E. C. Zipf, J. Chem. Phys. **55**, 5582 (1971).
[86]D. S. Newman, M. Zubek, and G. C. King, J. Phys. B **16**, 2247 (1983).
[87]J. C. Nickel and S. Trajmar (private communications, 1984).
[88]N. Oda and T. Osawa, J. Phys. B **14**, L563 (1981).
[89]S. Ohshima, T. Kondow, T. Fukuyama, and K. Kuchitsu, Chem. Phys. **85**, 403 (1984).
[90]K. Onda, J. Phys. Soc. Jpn. **54**, 4544 (1985).
[91]K. Onda and A. Temkin, Phys. Rev. A **28**, 621 (1983).
[92]K. Onda and A. Temkin, in preparation. (Preliminary results are reported in XIII ICPEAC Abstracts of Contributed Papers, p. 235.)
[93]K. Onda and D. G. Truhlar, J. Chem. Phys. **71**, 5107 (1979).
[94]K. Onda and D. G. Truhlar, J. Chem. Phys. **72**, 5249 (1980).
[95]C. B. Opal, E. C. Beaty, and W. K. Peterson, At. Data **4**, 209 (1972).
[96]D. Rapp and P. Englander-Golden, J. Chem. Phys. **43**, 1464 (1965).
[97]D. Rapp, P. Englander-Golden, and D. D. Briglia, J. Chem. Phys. **42**, 4081 (1965).
[98]J. R. Rumble, Jr., D. G. Truhlar, and M. A. Morrison, J. Chem. Phys. **79**, 1846 (1983).
[99]J. A. R. Samson, G. N. Haddad, and J. L. Gardner, J. Phys. B **10**, 1749 (1977).
[100]J. A. Schiavone, S. M. Tarr, and R. S. Freund, J. Chem. Phys. **70**, 4468 (1979).
[101]G. J. Schulz, Rev. Mod. Phys. **45**, 423 (1973).
[102]G. J. Schulz, in *Principles of Laser Plasmas*, edited by G. Bekefi (Wiley, New York, 1976), p. 33.
[103]M. Shaw and J. Campos, J. Quant. Spectrosc. Radiat. Transf. **30**, 73 (1983).
[104]D. E. Shemansky and A. L. Broadfoot, J. Quant. Spectrosc. Radiat. Transf. **11**, 1401 (1971).
[105]I. Shimamura, Chem. Phys. Lett. **73**, 328 (1980).
[106]*Electron–Molecule Collisions*, edited by I. Shimamura and K. Takayanagi (Plenum, New York, 1984).
[107]T. W. Shyn, Phys. Rev. A **27**, 2388 (1983).
[108]T. W. Shyn and G. R. Carignan, Phys. Rev. A **22**, 923 (1980).
[109]V. V. Skubenich and I. P. Zapesochnyy, Geomag. Aeron. **21**, 355 (1981).
[110]B. N. Srivastava and I. M. Mirza, Phys. Rev. **168**, 86 (1968).
[111]S. K. Srivastava, A. Chutjian, and S. Trajmar, J. Chem. Phys. **64**, 1340 (1976).
[112]P. N. Stanton and R. M. St. John, J. Opt. Soc. Am. **59**, 252 (1969).
[113]K. Stephan, H. Helm, and T. D. Märk, J. Chem. Phys. **73**, 3763 (1980).
[114]D. E. Stogryn and A. P. Stogryn, Mol. Phys. **11**, 371 (1966).
[115]S. N. Suchard and J. E. Melzer, *Spectroscopic Data, Vol. 2: Homonuclear Diatomic Molecules* (IFI/Plenum, New York, 1976).
[116]K. Takayanagi, in *Electron-Molecule Collisions and Photoionization Processes*, edited by V. McKoy, H. Suzuki, K. Takayanagi, and S. Trajmar (Verlag Chemie International, Deerfield Beach, 1983), p. 133.
[117]K. Takayanagi and T. Takahashi, Bull. Inst. Space Aeron. Sci. **2**, 1309 (1966) (in Japanese).
[118]H. Tanaka, L. Boesten, and I. Shimamura, in *7th ICAP Book of Abstracts*, 1980, p. 43, and private communications.
[119]H. Tanaka, T. Yamamoto, and T. Okada, J. Phys. B **14**, 2081 (1981).
[120]T. Taniguchi, H. Tagashira, and Y. Sakai, J. Phys. D **11**, 1757 (1978).
[121]P. R. Taylor, Mol. Phys. **49**, 1297 (1983).
[122]A. Temkin, Phys. Rev. A **17**, 1232 (1978); **18**, 783(E) (1978).
[123]S. Trajmar and D. C. Cartwright, in *Electron-Molecule Interactions and Their Applications*, edited by L. G. Christophorou (Academic, New York, 1984), Vol. 1, p. 155.
[124]S. Trajmar, D. F. Register, and A. Chutjian, Phys. Rep. **97**, 219 (1983).
[125]D. G. Truhlar, M. A. Brandt, A. Chutjian, S. K. Srivastava, and S. Trajmar, J. Chem. Phys. **65**, 2962 (1976).
[126]D. G. Truhlar, M. A. Brandt, S. K. Srivastava, S. Trajmar, and A. Chutjian, J. Chem. Phys. **66**, 655 (1977).
[127]L. Wallace, Astrophys. J. Suppl. **6**, 445 (1962).
[128]L. Wallace, Astrophys. J. Suppl. **7**, 165 (1962).
[129]W. C. Wells, W. L. Borst, and E. C. Zipf, Phys. Rev. A **14**, 695 (1976).
[130]H.-J. Werner, J. Kalcher, and E.-A. Reinsch, J. Chem. Phys. **81**, 2420 (1984).
[131]J. B. West, A. C. Parr, B. E. Cole, D. L. Ederer, R. Stockbauer, and J. L. Dehmer, J. Phys. B **13**, L105 (1980).
[132]G. R. Wight, M. J. van der Wiel, and C. E. Brion, J. Phys. B **9**, 675 (1976).
[133]H. F. Winters, J. Chem. Phys. **44**, 1472 (1966).
[134]S. F. Wong and L. Dubé, Phys. Rev. A **17**, 570 (1978).
[135]C. F. Wong and J. C. Light, Phys. Rev. A **30**, 2264 (1984).
[136]G. D. Zeiss, W. J. Meath, J. C. F. MacDonald, and D. J. Dawson, Can. J. Phys. **55**, 2080 (1977).
[137]E. C. Zipf and M. R. Gorman, J. Chem. Phys. **73**, 813 (1980).